PERFORMANCE AND SAFETY ANALYSIS OF A GENERIC SMALL MODULAR REACTOR

A Thesis

by

EVANS DAMENORTEY KITCHER

Submitted to the Office of Graduate Studies of
Texas A&M University
in partial fulfillment of the requirements for the degree of

MASTER OF SCIENCE

Approved by:

Chair of Committee,	Sunil Chirayath
Committee Members,	Pavel Tsvetkov
	Devesh Ranjan
Head of Department,	Yassin Hassan

December 2012

Major Subject: Nuclear Engineering

ABSTRACT

The high and ever growing demand for electricity coupled with environmental concerns and a worldwide desire to shed petroleum dependence, all point to a shift to utilization of renewable sources of energy. The under developed nature of truly renewable energy sources such as, wind and solar, along with their limitations on the areas of applicability and the energy output calls for a renaissance in nuclear energy. In this second nuclear era, deliberately small reactors are poised to play a major role with a number of Small Modular Reactors (SMRs) currently under development in the U.S.

In this work, an SMR model of the Integral Pressurized Water Reactor (IPWR) type is created, analyzed and optimized to meet the publically available performance criteria of the mPower SMR from B&W.

The Monte Carlo codes MCNP5/MCNPX are used to model the core. Fuel enrichment, core inventory, core size are all variables optimized to meet the set goals of core lifetime and fuel utilization (burnup). Vital core behavior characteristics such as delayed neutron fraction and reactivity coefficients are calculated and shown to be typical of larger PWR systems, which is necessary to ensure the inherent safety and to achieve rapid deployment of the reactor by leveraging the vast body of operational experience amassed with the larger commercial PWRs.

Inherent safety of the model is analyzed with the results of an analytical single channel analysis showing promising behavior in terms of axial and radial fuel element temperature distributions, the critical heat flux, and the departure from nucleate boiling ratio.

The new fleet of proposed SMRs is intended to have increased proliferation resistance (PR) compared to the existing fleet of operating commercial PWRs. To quantify this PR gain, a PR analysis is performed using the Proliferation Resistance Analysis and Evaluation Tool for Observed Risk (PRAETOR) code developed by the Nuclear Science and Security Policy Institute at Texas A&M University. The PRAETOR code uses multi-attribute utility analysis to combine 63 factors affecting the PR value of a facility into a single metric which is easily comparable. The analysis compared hypothetical spent fuel storage facilities for the SMR model spent fuel assembly and one for spent fuel from a Westinghouse AP1000. The results

showed that from a fuel material standpoint, the SMR and AP1000 had effectively the same PR value. Unable to analyze security systems and methods employed at specific nuclear power plant sites, it is premature to conclude that the SMR plants will not indeed show increased PR as intended.

DEDICATION

To my parents, Paul and Caroline, I would not be where I am today without you.

ACKNOWLEDGEMENTS

I would like to thank my Committee Chair, Dr Sunil S. Chirayath for always being available, giving insights and guidance in all aspects of the research and providing an environment where I have grown and matured upon arriving at Texas A&M University. He is an excellent academic, and a true gentleman.

I want to thank my Committee Members, Dr. Tsvetkov and Dr. Ranjan, for their support throughout the course of the research.

Thanks to my friends and colleagues and the Nuclear Engineering department faculty and staff at Texas A&M University for making my time there a greatly rewarding one.

Finally, thanks to my family and loved ones for their encouragement, friendship and love.

NOMENCLATURE

BOP	Balance of Plant
BOL	Beginning of Life
BAR	Burnable Absorber Rod
CHF	Critical Heat Flux
DNBR	Departure from Nucleate Boiling
EOL	End of Life
IPWR	Integral Pressurized Water Reactor
LWR	Light Water Reactor
LOCA	Loss of Coolant Accident
LEU	Low Enriched Uranium
MAUA	Multi Attribute Utility Analysis
PWR	Pressurized Water Reactor
PR	Proliferation Resistance
SCA	Single Channel Analysis
SMR	Small Modular Reactor

TABLE OF CONTENTS

Page

Page

LIST OF FIGURES

Page

Page

LIST OF TABLES

Page

1. INTRODUCTION

The high and ever growing demand for electricity coupled with environmental concerns (IAEA, 2007) and a worldwide desire to shed petroleum dependence, all point to a shift to utilization of renewable sources of energy. The under developed nature of truly renewable energy sources such as, wind, solar, and the associated concerns regarding the limitations on applicability and the energy output calls for a renaissance in nuclear energy. In this second nuclear era, deliberately small reactors (Ingersoll, 2009) are poised to play a major role with a number of Small Modular Reactor (SMR) designs currently under development in the U.S. These SMRs offer numerous benefits including inherent safety features with passive heat removal capabilities, increased security and proliferation resistance with integrated safeguards as well as advantageous economics (Ingersoll, 2009) to both the end user of the electricity and the developer of the power plant as economies of scale gains are there to be taken compared to a large Pressurized Water Reactor (PWR).

Currently there are over 50 SMR designs being developed all over the world with the entire range of nuclear technologies utilized, thermal, epithermal and fast neutron spectrum reactors, light water, gas and liquid metal cooled reactors ranging from ~5MWe to the 300MWe limit by definition. Of these, the integral PWR design is the closest to deployment due to the vast operating experience with the full scale equivalents. Three designs developed in the U.S. have began licensing activities with the Nuclear Regulatory Commission (NRC) (USNRC, 2011); an SMR from Westinghouse SMR based on their AP1000 PWR technology, the NuScale SMR (NuScale) from NuScale Power Inc. and the mPower SMR (mPower) from Babcock and Wilcox. The system developed and analyzed in this thesis will be modeled based on available design specifications of one of the above three designs with estimations/assumptions made for any unavailable design information.

1.1. Small Modular Reactors

Small Modular Reactors are characterized not by their size, but rather by the fact that additional design options and advantages are taken by intentionally making the reactors small. The general classification for a small reactor is one that produces up to 300MWe. Under this classification there are a large number of existing reactors that could be classified as small reactors. However they would not be considered as SMRs. SMRs use their size to their advantage in order to achieve additional design objectives. These reactor designs stress safety, security and cost.

An example of a safety benefit of a deliberately smaller size would be the resulting decreased thermal power density of the core allowing for passive heat removal systems (natural circulation) to be employed during all accident scenarios eliminating the need for forced circulation pumps etc, which are indispensable components of the safety systems employed by existing reactors.

Placing the entire reactor containment underground is another design option achievable by having a deliberately small reactor. This leads to an additional barrier for the radiation source term in the case of a radioactive release; a safety benefit. This also provides additional protection from missile strikes and aircraft impact; a security benefit. These and other aspects all point to decreased costs as system components are eliminated for simpler systems driven by physical phenomena and plant safety and security enhanced.

The primary cost advantage offered by the deployment of SMRs however is the reduced the up-front capital costs to the developer. SMRs will have relatively low capital costs and the ability to meet a larger range of applications from base loads in high demand areas to implementation in developing and emerging grids (Ingersoll, 2009) incompatible to large 1000MWe reactors. Modularity benefits such as standardized core components that can be manufactured in a factory setting result in increased quality assurance and decreased plant construction times. Quantifying these and other potential benefits and giving the SMR the appropriate benefit, SMRs have been shown to be economically competitive with larger power reactors (Carelli et al, 2010).

1.2. Existing Pressurized Water Reactors

The Pressurized Water Reactor is a Light Water Reactor design operating with a thermal neutron spectrum and represents a large portion of commercial power plants worldwide. The primary coolant for the reactor is light water which also acts as the moderator. The fuel is usually low enriched uranium (LEU) in the uranium dioxide (UO_2) form, or occasionally mixed oxide containing both uranium dioxide and plutonium dioxide (UO_2+PuO_2). The coolant is kept from boiling and remains in single phase as a liquid in spite of the high temperatures (~300°C) by keeping it pressurized. The pressuriser maintains the primary coolant at pressures in the region of ~15MPa.Typical PWR power plants also use light water as the secondary coolant which passes through the steam generator producing super heated steam to drive the turbine(s) and produce electricity. Figure 1 shows a typical 4-loop PWR (Kok, 2009). The 4-loop PWR has four steam generators connected to one reactor core and one pressuriser with a coolant pump for each loop.

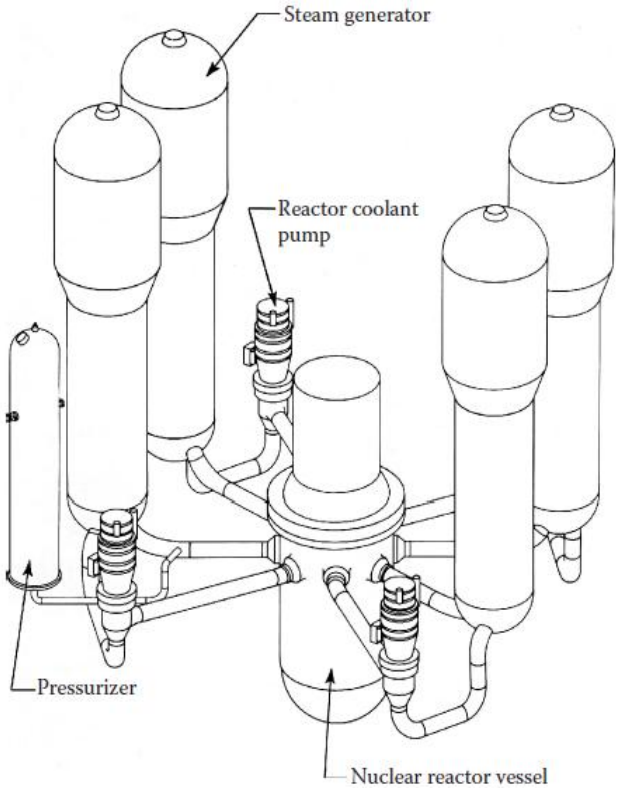

Figure 1: Typical Layout of a 4-loop PWR

1.3. Integral Pressurized Water Rectors

One of the major accident scenarios for a PWR is what is known as a large break loss of coolant accident or large-break LOCA. In this scenario, it is assumed that one of the large coolant pipes connecting the reactor core to the steam generators suffers a large double ended break. Such an event would lead to rapid uncovery of the core as a large fraction of the coolant inventory would be lost. This will eventually lead to a large scale radioactive fission source term release. As a result, a plethora of auxiliary safety systems had to be added to the design to ensure that in the case of the large-break LOCA, the core remained covered with coolant and heat removal systems remain capable of removing the remaining decay heat.

The Integral Pressurized Water Reactor (IPWR) takes a dramatic approach to mitigating this accident scenario. The IPWR design places the pressuriser, steam generator and coolant pump along with the core inside the same pressure vessel; thus eliminating the large coolant pipes and the associated possibility of a large-break LOCA all together. This can only be done in the case of SMRs as their smaller size and associated components makes forging a large enough pressure vessel possible.

The proposed SMRs that are near deployment are all of this type. Not only does this eliminate an entire category of accident scenarios but also increases the coolant inventory in the core allowing heat removal by natural circulation to be applicable over a wider range of operation. Such innovative and inherently safe design features are what characterizes SMRs. The SMR to be investigated will be of the IPWR type with a component layout envisioned to be similar to that of the mPower shown in Figure 2 (Shirvan et al., 2012.).

1.4. Design Objectives

The main application of the new fleet of SMRs will be for electricity generation. Although they can be used to replace coal fired plants producing <300MWe for base load purposes, their niche market and where they will come into their own is in rural/developing areas where the existing grid is not capable of bringing a single large 1000MWe plant online. Rather a series of eight individual SMRs producing 150-200MWe can be employed to meet

the same demand. The first module can be built immediately with additional units brought online in direct response to the growth of demand in the area.

The design will borrow many design parameters from the existing fleet of large PWRs in operation in the U.S. This occurs as a result of the desire to deploy these reactors in the near term. By leveraging heavily upon technologies used in the currently operating PWRs, the licensing and certification of the resulting IPWR SMR design will be easier; again with rapid deployment driving this objective. The SMR design is intended for a "battery type" deployment meaning there is no fuel assembly shuffling over the entire lifetime of the core's operation. Once the core can no longer maintain criticality, the entire core is removed and reprocessed offsite and replaced with a brand new core much like a replacing a depleted battery.

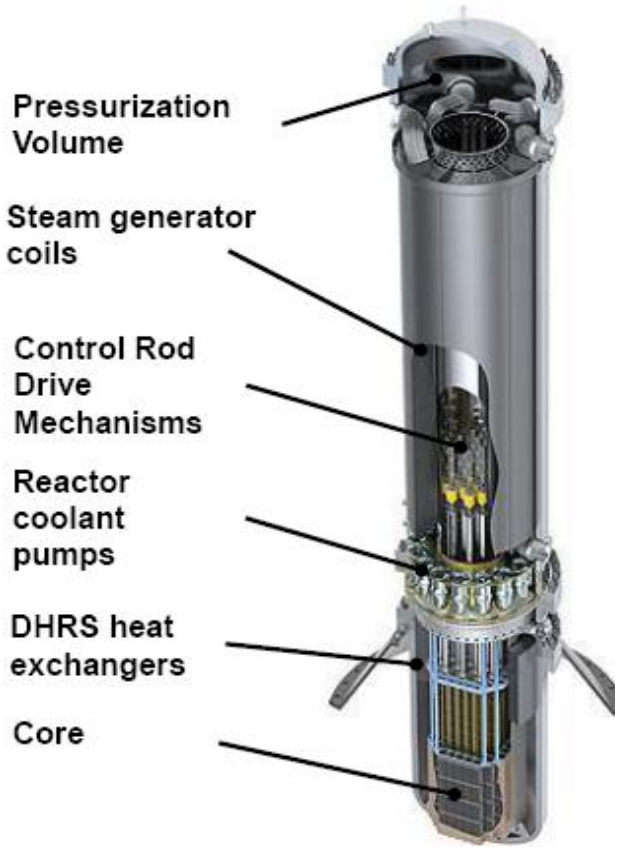

Figure 2: mPower Schematic Showing Layout of an Integral PWR

1.5. Thesis Objectives

This study will focus on developing a computational model based on the IPWR SMR design to match the performance characteristics proposed for the mPower SMR by B&W. The model will be analyzed for its performance with regards to meeting the desirable core characteristics, safety requirements regarding fuel temperatures and heat removal and a comparison of the Proliferation Resistance (PR) of the design to that of an existing large PWR.

This work will include:

1) the development of an MCNP5 (X-5 Monte Carlo Team, 2008) and MCNPX2.6 (Pelowitz, 2008) full core model of the proposed SMR design for neutronics assessment for
    a. Reactivity feedback coefficients – Doppler, Coolant Temperature and Void
    b. Reactor kinetics parameters - delayed Neutron fraction and mean generation time
    c. Burnup – Core lifetime and End Of Life (EOL) isotopic composition
    d. Core flux and power profiles for Peaking Factors – Axial and Radial
2) a thermal hydraulics single channel analysis (SCA) of the hottest fuel rod channel
    a. Temperature profiles – Radial and Axial temperature profiles in the hottest pin
    b. Critical Heat Flux and Departure from Nucleate Boiling Ratio
3) a PR assessment using the Proliferation Resistance Analysis and Evaluation Tool for Observed Risk (PRAETOR) code to compare the relative PR value to an existing large PWR (Giannangeli, 2007; Metcalf, 2009; Chirayath et al., 2010)

The results of these analyses will allow conclusions regarding the feasibility of the design, its performance characteristics and its proliferation resistance characteristics.

2. APPLIED CODES

The model development and analysis was largely done using MCNP5 and MCNPX; both general geometry radiation transport codes employing the Monte Carlo particle transport method. The MCNP5 and MCNPX codes were used to perform the reactor core physics calculations.

The thermal hydraulics single channel analysis of the hottest fuel channel is done completely analytically. This is done using Microsoft EXCEL and Simulink MATLAB.

The proliferation resistance analysis is done using the PRAETOR code, a proliferation risk assessment tool developed by Texas A&M University. PRAETOR will be used to compare the proliferation resistance of the SMR design evaluated in this thesis to an existing large PWR. ORIGEN-ARP is employed along with MCNP5/MCNPX to generate some of the inputs required for the PRAETOR code.

2.1. MCNP

The general purpose Monte Carlo N-Particle (MCNP) code can be used to handle neutron, photon and electron transport developed at Los Alamos National Laboratory. It is especially powerful due to its use of continuous energy cross-section data and ability to handle complex three-dimensional geometry. For reactor physics applications, MCNP offers important features such as user defined material composition and geometry using regions defined by unions, intersections and complements of the surfaces bounding the cell. Lattice structures allow for the definition of the fuel assembly and reactor core. For thermal neutron interactions, the option to treat the material as a free gas or apply the thermal scattering laws is available. The thermal scattering laws are especially important as they account for the effects on neutron scattering angle and energy due to the fact that at thermal energies, the target atom cannot be treated as a free gas but is in fact bound to a molecule. The various neutron flux tallies allow for flux spectra and neutron spatial distributions to be determined (X-5 Monte Carlo Team, 2008).

2.2. MCNPX

MCNPX, like MCNP5 is also a general geometry Monte Carlo code also developed at Los Alamos National Laboratory but with additional capabilities to track heavy charged particles over a wider range of particle energies. MCNPX was used mainly for its added ability to perform transmutation, activation and burnup calculations in reactor core physics simulations (Pelowitz, 2008). Burnup calculations are used to determine the lifetime of the reactor core; an important parameter for assessing core performance. The EOL isotopic composition, especially plutonium content, is also important and is a major factor in the PR assessment.

2.3. ORIGEN-ARP

ORIGEN-ARP is a depletion/burnup analysis sequence employed in the SCALE suite for spent fuel depletion, decay and source term analysis. The sequence calls the ORIGEN-S code which does the depletion calculations and the Automatic Rapid Processing (ARP) module to generate the required problem-specific cross section libraries. These libraries are generated by interpolation algorithms based on pre-generated libraries for a set of existing reactor types. Various methods are available to do this interpolation based on various problem parameters such as fuel enrichment, neutron fluence and burnup. User prescribed output data will provide information on the heat and radiation load of the material; all attributes required for the PR analysis with PRAETOR (Gauld et al. 2009).

2.4. PRAETOR

PRAETOR is a code developed to help in comparing the proliferation resistance of any facility having nuclear material that can be diverted to make a nuclear weapon. The code uses Multi Attribute Utility Analysis (MAUA) methodology to provide a single metric for the installation's PR value based on 63 different intrinsic and extrinsic attributes. This methodology basically provides a means to correctly weigh and fold down many influencing factors into a single number to facilitate decision making. The four stages of proliferation

evaluated within the code are Diversion, Transport, Transformation and Weapon Fabrication. The code assesses the installation at 3 different levels providing the utility values for each stage the sub-stages within. The 63 required inputs compose of values to be calculated using MCNP, MCNPX, and ORIGEN-ARP along with other country-specific parameters. The results for the SMR and PWR from PRAETOR will be assessed to determine their relative PR values.

3. REACTOR CONCEPT

The SMR design selected for the computational study is an integral PWR (IPWR) specified to produce 500MWth power for 150-200MWe assuming a secondary side efficiency of 30-40%. The desired core lifetime is four years. These desired design parameters drove the development of the SMR model and the optimization of the other relevant parameters.

3.1. Existing PWR Assembly Parameters

As mentioned in the design objectives, there are a host of technology transfers from existing large PWRs to the SMR design in order to facilitate licensing and promote safety through over half a century of operating experience. The SMR fuel assemblies are to be exactly the same as the typical existing large PWR with respect to materials and dimensions except for the active fuel length. As such a typical 17x17 fuel assembly configuration was chosen. Figure 3 shows the geometry of a single fuel cell as modeled in MCNP. The fuel assembly parameters used in the model were kept the same as the existing large PWR and are presented in Table 1 (Kok, 2009).

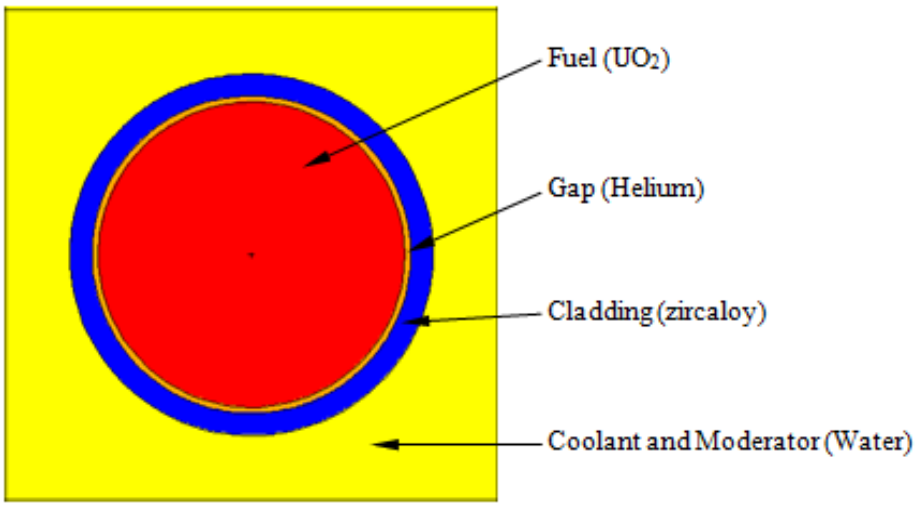

Figure 3: PWR Fuel Pin Geometry Used for the SMR

Table 1: PWR Fuel Assembly Details Used for the SMR Assembly

Fuel Rod Parameters	Value
Fuel Material	UO_2
Fuel Enrichment	Various (All <5%)
Active Fuel Length*	Reduced for the SMR
Fuel Pellet Diameter (cm)	0.784352
Gap Material	Helium
Gap Outer Diameter (cm)	0.815848cm
Clad Material	Zircaloy-4
Clad Outer Diameter (cm)	0.930148cm
Fuel Lattice Pitch (cm)	1.25984cm
Assembly size	17x17
Fuel rods per assembly	264
Guide tubes	25
Fuel assemblies in the core*	Reduced for the SMR

3.2. Fuel Enrichment

The fuel material is low enriched uranium (LEU) uranium dioxide (UO_2). Typical PWR cores will have fuel assemblies with a range of uranium enrichment levels. For use in commercial reactors, LEU is enriched to between 3 and 5% ^{235}U. The fuel rod consists of low enriched UO_2 pellets with a helium gap and zirconium alloy cladding. The active fuel length, fuel enrichments and loading pattern are all unknown and will be investigated and optimized in order to achieve the desired power for the envisaged four year core lifetime. As a result, core size is also a variable.

3.3. Active Fuel Length and Height-to-Diameter Ratio

The desired design feature of smaller core size necessitates a reduction in the active fuel length parameter when compared to the PWR and likewise the reduction in total core power results in reducing the number of assemblies comprising the core. Thus steps had to be taken to achieve a viable SMR assembly height and SMR core size.

When decreasing the fuel assembly height, two parameters were considered; the core height-to-diameter ratio and the infinite neutron multiplication factor (k_∞) of the SMR assembly.

From nuclear reactor theory, assuming one-group diffusion, it can be shown that a height-to-diameter ratio of approximately 1 is the optimal configuration to reduce leakage from a bare homogenous cylindrical core once the material choices for the SMR are assumed. Though the SMR core is neither a true cylinder, homogenous nor bare, it can be assumed as such and the general principle remains true to a large extent. The active core diameter is discrete in nature as it is a function of the number of assemblies used in the core, this value is determined later. The maximum allowable value for this ratio is set to 1.1 as a design constraint. The AP1000, a new PWR design developed by Westinghouse, has an active cold fuel length of 426.72cm and an equivalent core diameter of 304.038cm (Westinghouse, 2003a) for a Height-to-Diameter ratio as high as 1.4.

The consideration for the infinite multiplication factor was to investigate how it scales with height with the aim to keep the value of this parameter the same for both the full size PWR assembly and the reduced height SMR assembly. The end result should be that the reactivity and kinetics characteristics of the SMR core should remain similar to that of the PWR, which are well understood and for which control mechanisms and procedures are well developed. The desired core lifetime and hence required fuel loading is also a factor.

In order to see the effect of reducing the height of the fuel assembly on the infinite multiplication factor, a single fuel assembly was modeled from the fuel pin cell details given in Table 1 and Figure 3. Enrichment was set at 3% ^{235}U; the average core enrichment for the PWR. The assembly was modeled using reflecting boundary conditions on the x and y sides with approximately 25cm of water above and below the assembly to simulate axial reflection in water. The fuel meat height was varied. Structural components of the assembly were not

modeled as they have little effect on the neutronics behavior. Figure 4 shows axial and radial cross-sections of the model used to perform the height-to-diameter analysis.

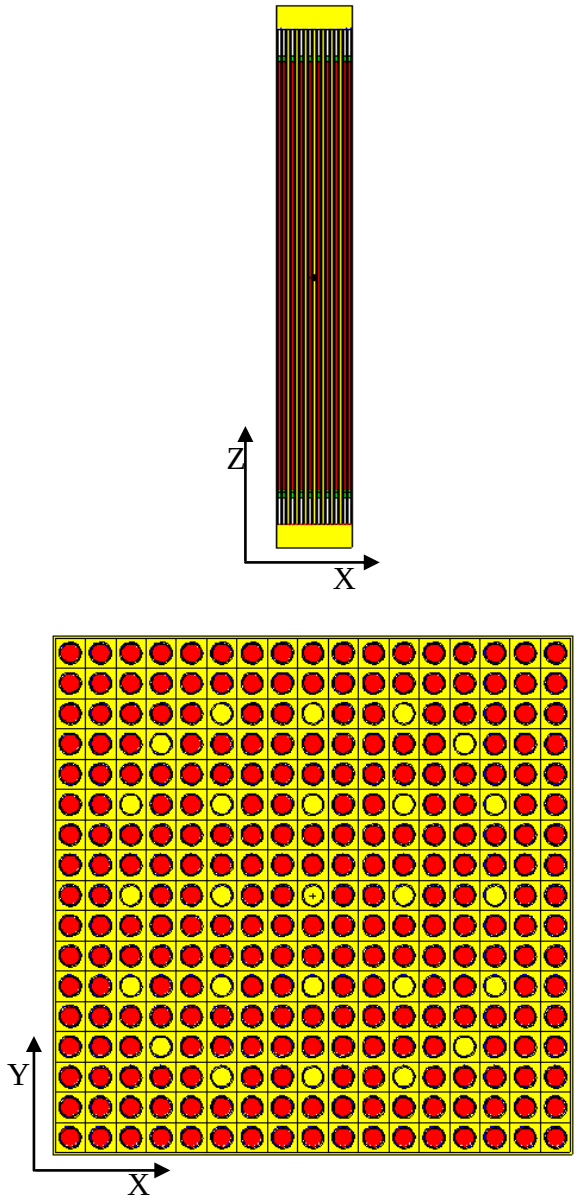

Figure 4: Radial and Axial Cross-sections of a Single Fuel Assembly

The results for the infinite multiplication factor as a function of active fuel length is presented in Table 2. The resulting plot, Figure 5, shows clearly that below an active fuel

length of approximately 180cm, the infinite multiplication factor begins to drop rapidly. The effective multiplication factor for the finite core will be less than what is predicted for the infinite lattice as there are leakage effects that have been ignored by having the reflecting boundary conditions in the assembly level model. Based on this information, 180cm is set as the minimum fuel length for the design; where$k_\infty = k_{inf} = 1.32$.

Table 2: Infinite Multiplication Factor (k_{inf}) as a Function of Active Fuel Length

Actual Fuel Length (cm)	Reduction in Height (cm)	Infinite Multiplication Factor k_∞
365.76	0	1.33421
345.76	20	1.33363
325.76	40	1.33320
305.76	60	1.33197
285.76	80	1.33106
265.76	100	1.32989
245.76	120	1.32882
225.76	140	1.32587
205.76	160	1.32380
185.76	180	1.32059
165.76	200	1.31621
145.76	220	1.31088
125.76	240	1.30317
105.76	260	1.29193
85.76	280	1.27278
65.76	300	1.24279
45.76	320	1.18585
25.76	340	1.05920
5.76	360	0.66981

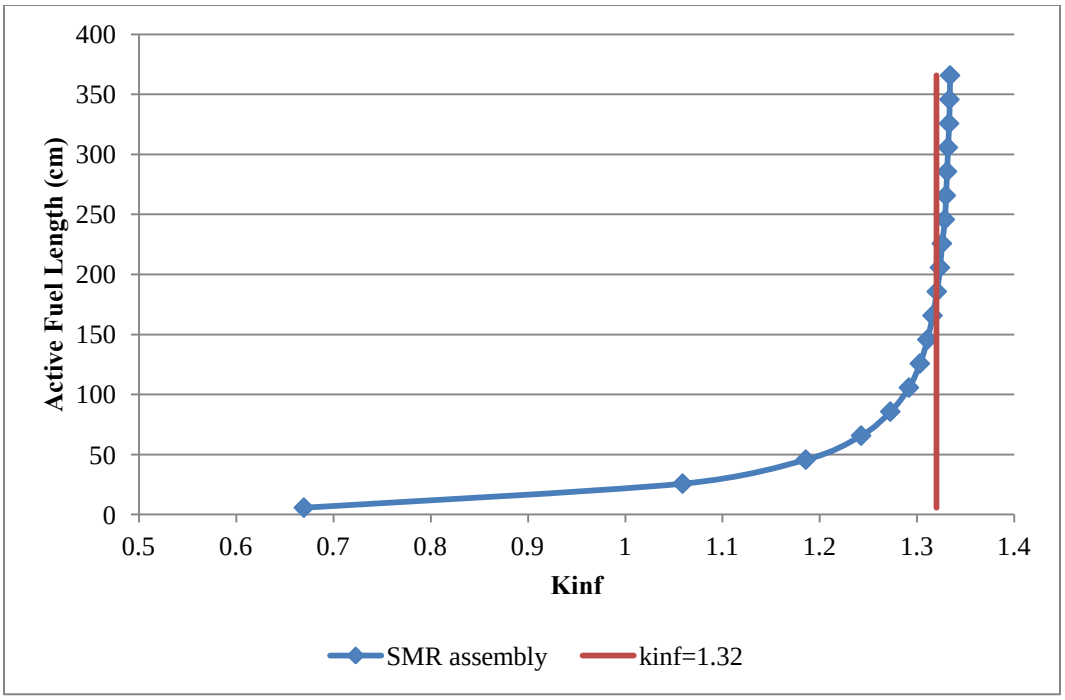

Figure 5: Infinite Multiplication Factor (k_{inf}) as a Function of Active Fuel Length

3.4. Core Size

The core size can now be determined. From the assembly parameters defined above and the desired core performance characteristics of 500MWth for four years, an estimate for the amount of uranium needed can be calculated. The simple equation for burnup is used.

$$Burnup = \frac{Power \times Time \times Capacity\ Factor}{Mass\ of\ Uranium}$$

$$BU = \frac{P \times t \times CF}{MTU}$$

The final discharge burnup of the fuel at EOL is limited by the fact that core shuffling will not be employed. A fuel burnup target of 40gigawatt days per metric ton of uranium (40GWd/MTU) is set. This is relatively low considering that the average burnup of existing large PWRs is around 50-55GWd/MTU with the AP1000 average discharge burnup as high as 60GWd/MTU (Westinghouse, 2003b).

The required mass of uranium is found to be 18.25MT.

$$MTU = \frac{P \times t \times CF}{BU}$$

$$MTU = \frac{500MWth \times 4 \times 365days \times 1}{40000MWd/MTU} = 18.25MTU$$

Then knowing the mass of uranium per assembly, the required number of assemblies to make the core is easily calculated. Figure 6 shows that the number of assemblies required lies between 80 and 35 for the range of active fuel lengths between the full size PWR assembly (365.78cm) and the infinite multiplication factor limit (180cm).

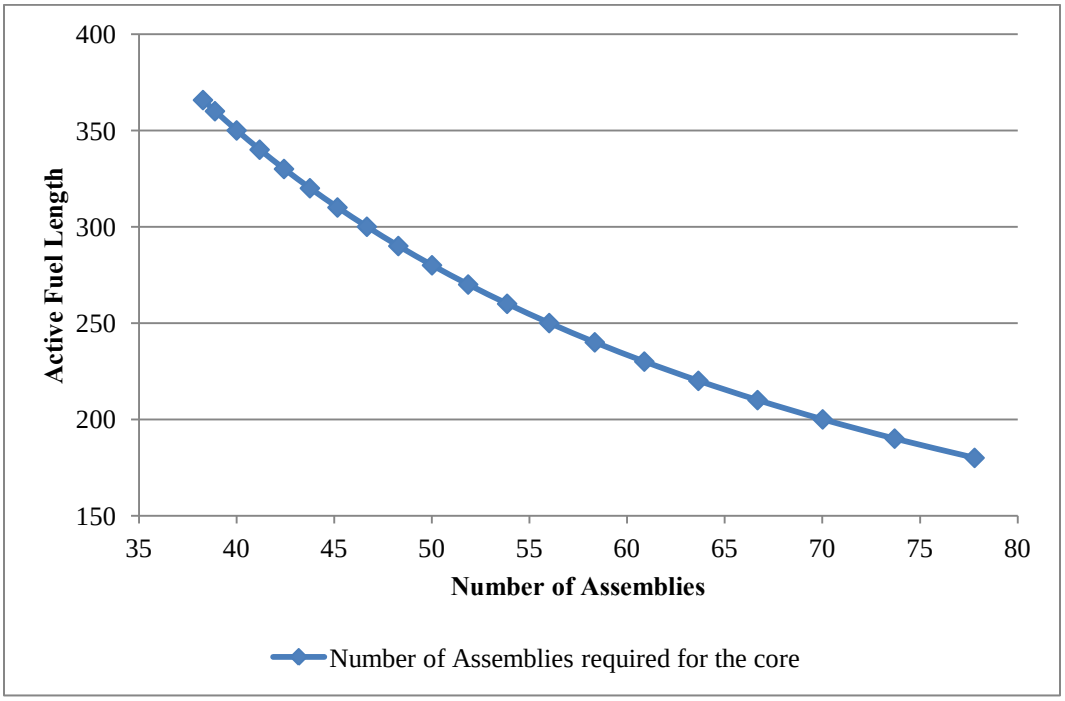

Figure 6: No. of Assemblies in the SMR Core as a Function of Active Fuel Length

A uniform power distribution is a desirable feature of commercial reactors. This can be largely achieved by having symmetric core geometry. Figure 7 shows the feasible core layouts with each yellow square representing a fuel assembly position, each white square

representing water filled positions and the concentric rings show the general radial nature of the flux. There are only five such layouts within the 35-80 assembly range defined earlier. From the figure, it can be seen that there are only two options for the core diameter; seven assemblies in the mid-plane or nine assemblies in the mid-plane. These configurations correspond to cores having diameters of 151.32096cm (radius = 75.66048cm) and 194.55552cm (radius = 97.27776cm) respectively.

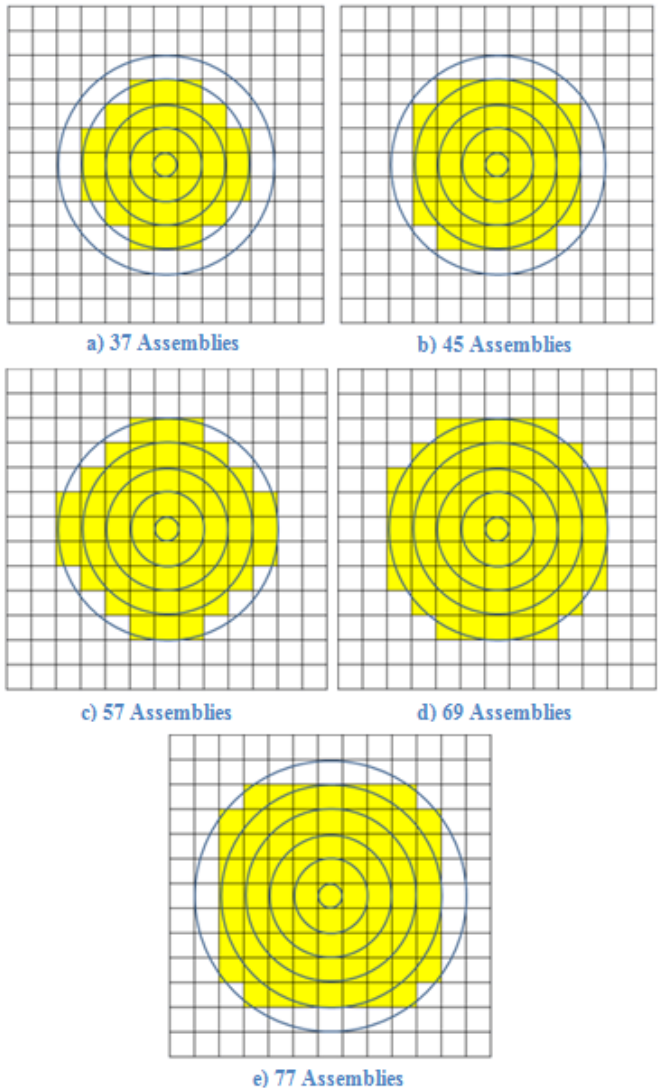

Figure 7: Feasible Core Layouts

Taking into account the height-to-diameter ratio requirement and the 180cm active fuel length minimum, it was found that all core layouts with 7 assemblies in the mid plane were unacceptable (Figure 7.a and Figure 7.b).

Table 3 and Figure 8 show the results of the height-to-diameter ratio analysis. Thus three viable core layouts remain. Knowing the fuel pin dimensions, the fuel material density and total required mass of uranium required for the initial core loading, the required fuel lengths for each of these configurations were determined. Table 4 shows the results of the analysis. Subsequently, core layouts with 57 assemblies (Figure 7.c) and 77 assemblies (Figure 7.e), were also discarded.

Table 3: Core H/D Values as a Function of Active Fuel height

Active Fuel Length (H) (cm)	Height-to-Diameter Ratio for D=151.32096cm (7 Assemblies in the Mid-plane)	Height-to-Diameter Ratio for D=194.55552cm (9 Assemblies in the Mid-plane)
180	1.189524571	0.925185777
190	1.255609269	0.976584987
200	1.321693968	1.027984197
210	1.387778666	1.079383407
220	1.453863364	1.130782617
230	1.519948063	1.182181827
240	1.586032761	1.233581036

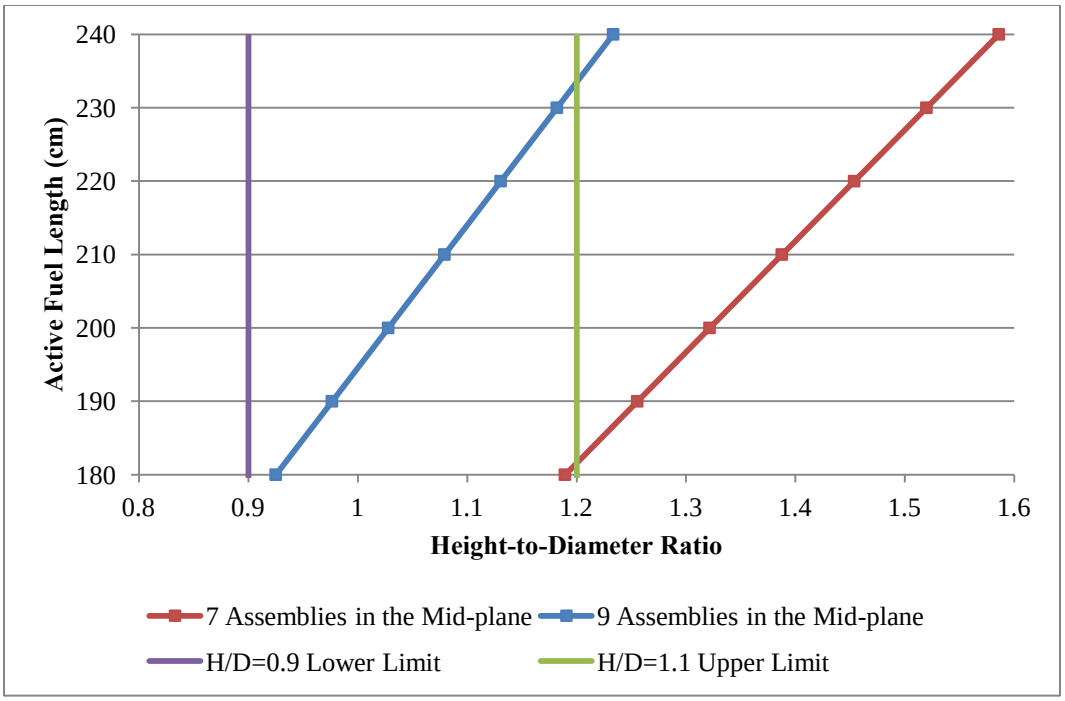

Figure 8: Resulting Core H/D Values as a Function of Active Fuel height

Table 4: Required Fuel Lengths and Core H/D Values for Various Core Layouts

Number of Assemblies	Required Fuel Length (H) (cm)	Resulting Diameter (D) (cm)	Resulting H/D ratio
37	378.541	151.32096	2.50
45	311.245	151.32096	2.05
57	245.716	194.55552	1.26
69	202.986	194.55552	1.04
77	181.897	194.55552	0.93

The core layout having 69 assemblies (Figure 7.d) was chosen for the rest of the analysis. The corresponding required fuel length is 202.986. An active fuel length of 200cm is used for ease of computations. Figure 9 shows axial and radial cross-sections of the model as developed in MCNP5.

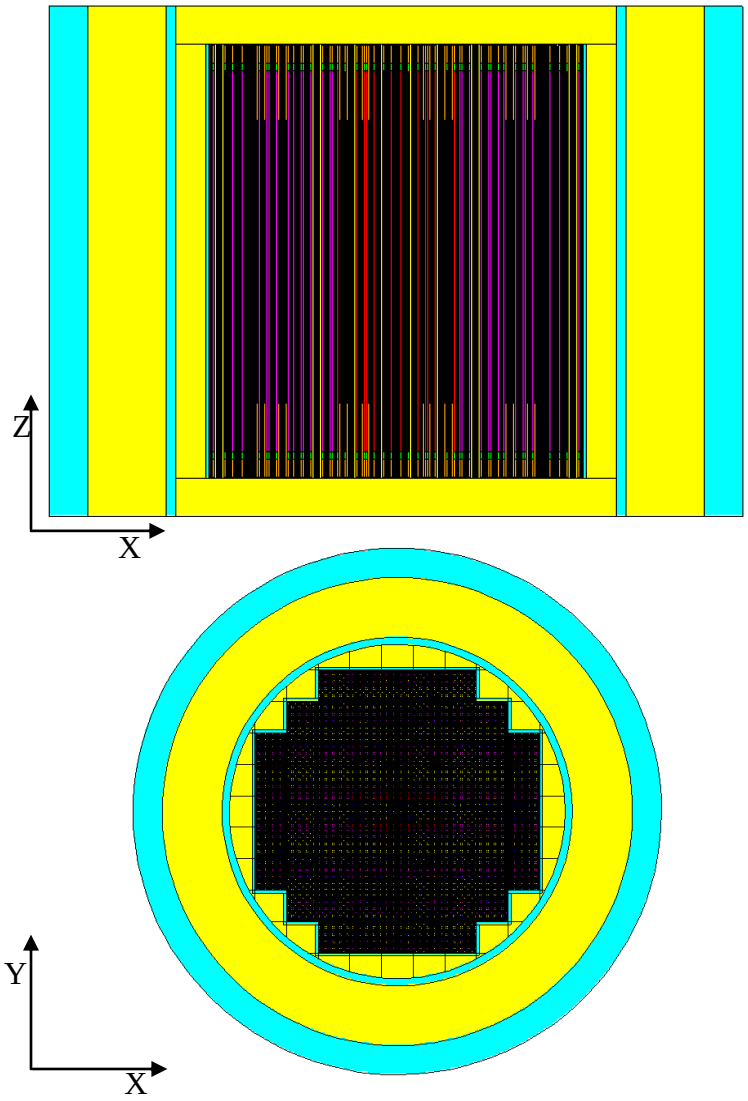

Figure 9: Axial and Radial Cross-sections of the SMR Model

3.5. Reactivity Control

The initial core loading would have Burnable Absorber Rods (BARs) made out of B_4C to aid with flattening the neutron flux and hence core power profiles to reduce power peaking and also to achieve uniform fuel burnup. This is also a technique employed by existing large PWRs. PWRs also incorporate fuel integral BARs. This is not done in the SMR core. The absorber material is natural boron carbide (B_4C) with 19.9% ^{10}B.

In addition to BARs and control rods, existing large PWRs use soluble boron in the coolant/moderator as a means of controlling core reactivity. The reactivity control in the SMR would be entirely through the manipulation of control rods. There is no soluble boron in the light water coolant/moderator of the SMR. Figure 10 shows a radial cross-section of a BAR rod.

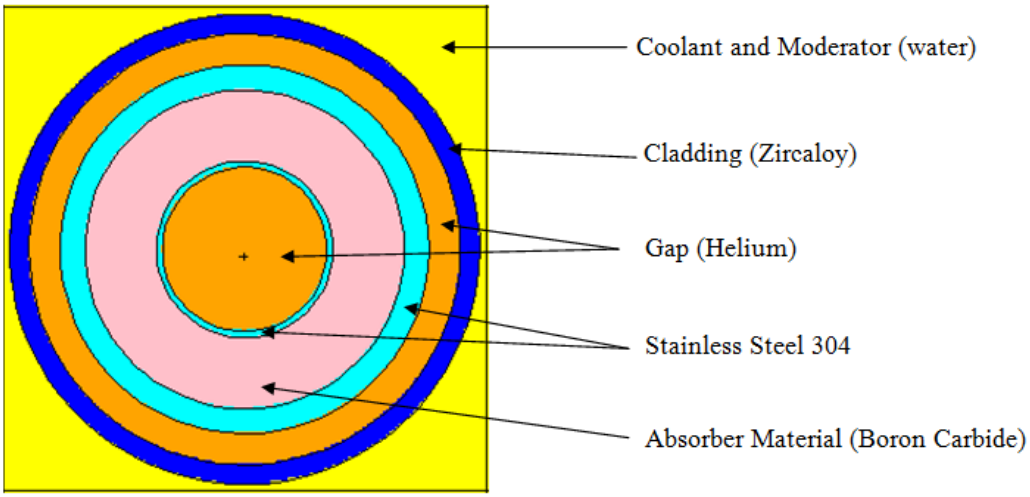

Figure 10: Radial Cross-section of the BAR

3.6. Core Loading Pattern and Shuffling

The target core life time for the SMR is four years, under the "battery type" refueling regime with no core shuffling. All existing commercial PWR's employ some sort of fuel assembly shuffling regime whereby each fuel assembly sees multiple irradiation cycles in the core at different locations. Core shuffling increases fuel burnup and increases core lifetime while at the same time minimizing core peaking. At each shuffling step a potion of the core is discarded and replaced by adding fresh fuel. Figure 11 shows a typical core loading pattern for a PWR employing 3 different assemblies with different fuel enrichment (Kok, 2009). Without shuffling the fuel assemblies within the core, achieving respectable levels of burnup and the target four year lifetime while minimizing power peaking will be a challenge for the SMR core.

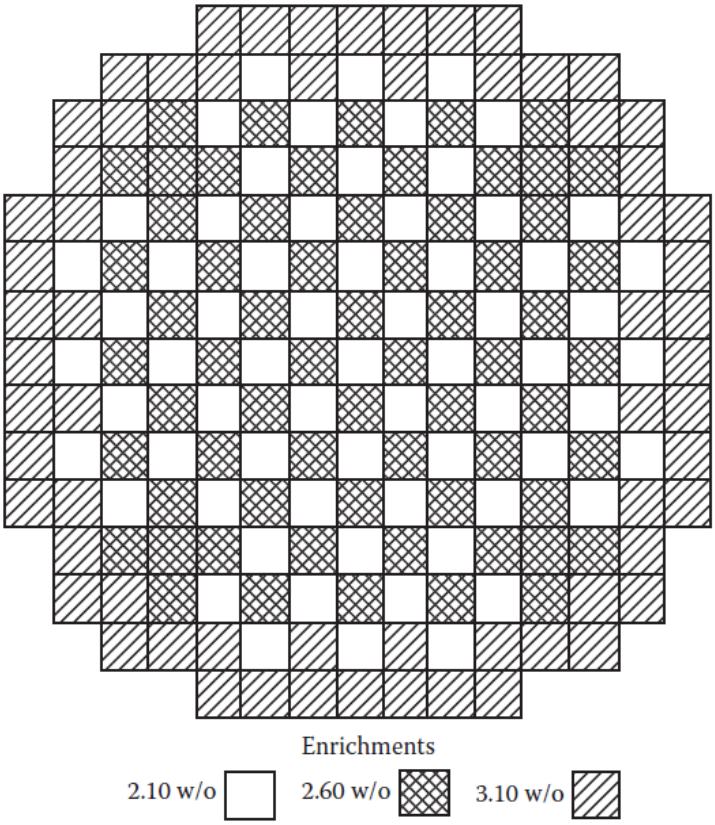

Figure 11: Typical Checked Core Loading Pattern for a PWR

3.7. Balance of Plant

The SMR is designed for the purpose of electricity generation operating on the Rankine cycle. The Balance of Plant (BOP) consists of the same components found at a commercial PWR, namely a steam generator (in this case integral to the reactor pressure vessel), a steam turbine and compressor. Design and analysis of this component of the SMR plant is outside the scope of work for this thesis.

4. REACTOR ANALYSIS

With much of the reactor conceptual design well developed, analysis will focus on optimizing and determining operational characteristics of the core. Several design choices have been already made, employing existing technologies and taking advantage of operational experience to promote immediate development, certification, licensing and deployment. At this stage, fuel assembly dimensions have been set with active fuel length set to 200cm for the initial analysis. The core now has finite dimensions and as such the reflective boundary conditions employed for the assembly level calculations are discarded. The neutron multiplication factor now becomes the effective multiplication factor (k_{eff}).

From core leakage and initial uranium loading considerations, a core layout of 69 assemblies has been settled upon. The fuel is uranium dioxide fuel (UO_2) with a maximum enrichment of 5% ^{235}U. The actual fuel enrichment(s) remains to be found.

Depletion calculations will be performed to find a core loading that is capable of producing the desired 500MWth for four years (1440days). An investigation into the required BAR loading pattern is required to reduce the reactivity swing over the core lifetime and also reduce power peaking. This core will again be depleted to see the penalty in core lifetime due to employing BARs.

4.1. Required Fuel Enrichment

At this stage, the total volume of fuel in the core has been set by fixing the dimensions and number or fuel assemblies in the core. Thus fuel enrichment becomes the driving force as far as core lifetime is concerned. The enrichment schemes used by existing large PWRs employing fuel assemblies of varying enrichments were retained. Two different enrichments will be used. The highest enrichment level in the core is here referred to as the primary enrichment (PE). The secondary enrichment (SE) is the lower enrichment level.

In order to investigate the level of fuel enrichment required, four cores were modeled and depletion calculations performed using MCNPX. These configurations had core wide

enrichments of 3.6, 4.0, 4.4 and 4.8% ^{235}U. These scoping simulations set the maximum achievable lifetimes for a core having that level of primary enrichment.

Table 5: Effective Multiplication Factor for Cores with Various Primary Enrichment

	Effective Multiplication Factor (k_{eff}) for various Primary Enrichments				
Time (days)	3.6%	4.0%	4.4%	4.8%	5.0%
0	1.32156	1.33794	1.35785	1.36978	1.37855
90	1.24606	1.26406	1.27959	1.29647	1.30599
180	1.21306	1.23570	1.25539	1.27130	1.27771
270	1.18343	1.20712	1.22957	1.24482	1.25300
360	1.15757	1.18266	1.20017	1.22154	1.23029
450	1.13339	1.15771	1.17740	1.19906	1.20499
540	1.10857	1.13223	1.15577	1.17514	1.18481
630	1.08663	1.11131	1.13558	1.15410	1.16395
720	1.06310	1.09064	1.11269	1.13357	1.14515
810	1.04112	1.06976	1.08976	1.11281	1.12365
900	1.01716	1.04674	1.07078	1.09588	1.10449
990	0.99685	1.02618	1.05074	1.07494	1.08650
1080	0.97537	1.00774	1.03314	1.05597	1.06683
1170	0.95863	0.98594	1.01349	1.03815	1.04764
1260	0.93827	0.96684	0.99220	1.01801	1.02895
1350	0.91933	0.94840	0.97649	1.00143	1.01180
1440	0.90224	0.93074	0.95648	0.98212	0.99412

The actual core would replace PE assemblies with SE assemblies and add some BARs. Both these changes will reduce core lifetime. Thus if these scoping runs were unsuccessful, a core with this level of primary enrichment was discarded. Table 5 shows the results of this analysis. The cells shaded yellow, show the last burn step at which the effective multiplication factor (keff) remained above one. Once keff drops below one, the core can no longer remain critical and is in effect spent. At this point refueling is necessary.

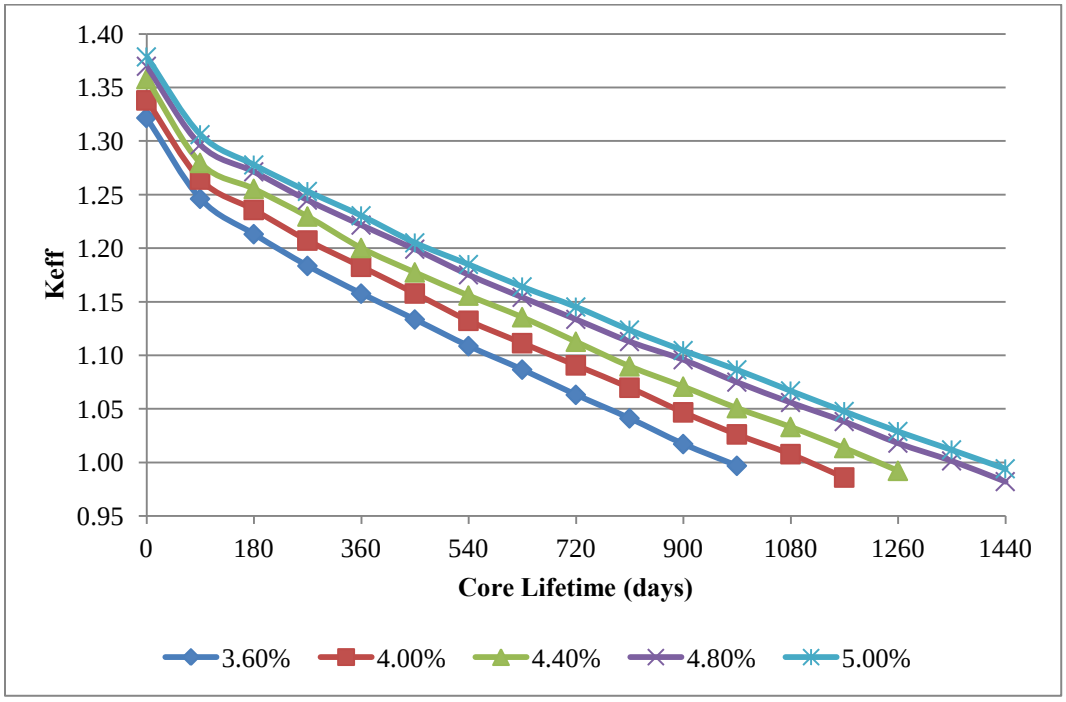

Figure 12: k_{eff} vs. Core Lifetime for Various Primary Enrichments

From Figure 12, it is clear that only the cores having primary enrichments of 4.8% ^{235}U and 5.0% ^{235}U have the potential of attaining the desired four year (1440days) core lifetime. Regardless of the scoping simulations suggesting sub-criticality at 1440days, methods exist to stretch the lifetime of the core by the deficient 90days. The 4.8% ^{235}U enriched case is taken forward for further investigation into whether the target lifetime can be achieved even after losses due to the replacement of PE assemblies with lower SE assemblies and the addition of BARs. The 5.0% ^{235}U enriched case remains a fall back option should this

target prove unachievable. Higher fuel enrichment results in higher fuel costs. Taking these economic concerns into consideration, the lowest possible PE and SE levels at which the SMR targets are achieved is desirable.

4.2. Effect of Secondary Enrichment Assemblies

Secondary enrichment assemblies will be placed at the centre of the core such that the higher flux available will compensate for the lower enrichment to produce the same amount of power as in the primary enrichment assemblies having a higher enrichment.

In order to determine the effect of this decrease in enrichment in the centre of the core, two test cases were done. The first case involved replacing 5 assemblies and the second case involved replacing 9 assemblies. The results for these calculations are shown in Table 6 and Figure 13.

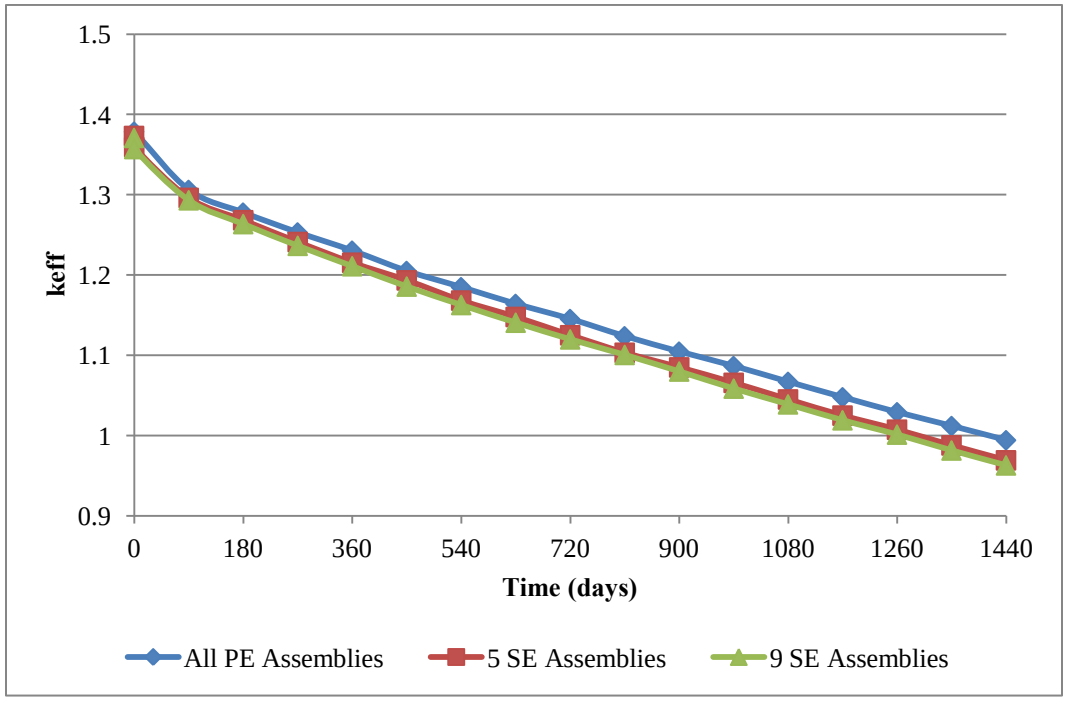

Figure 13: Effect of SE Assemblies on Core Lifetime

Table 6: Effect of SE Assemblies on Effective Multiplication Factor (k_{eff})

Time (days)	All PE Assemblies	5 SE Assemblies	9 SE Assemblies
0	1.37855	1.37326	1.3708
90	1.30599	1.29607	1.2931
180	1.27771	1.2683	1.26348
270	1.2530	1.24108	1.2364
360	1.23029	1.21531	1.21093
450	1.20499	1.19333	1.18564
540	1.18481	1.16818	1.16262
630	1.16395	1.14772	1.14059
720	1.14515	1.12496	1.11981
810	1.12365	1.10311	1.10044
900	1.10449	1.08488	1.07977
990	1.08650	1.06564	1.05846
1080	1.06683	1.04495	1.03885
1170	1.04764	1.02484	1.01899
1260	1.02895	1.00727	1.0012
1350	1.01180	0.98769	0.98139
1440	0.99412	0.96908	0.96279

It is clear from the data, that as expected the time period for which the core can maintain criticality is reduced by replacing primary enrichment assemblies. The 5-assemblies-replaced case resulted in a reduced effective neutron multiplication factor at end of life as did the 9-assemblies-replaced case; which caused a further reduction in effective neutron multiplication factor. The results suggest that a higher SE is required for both the 5% ^{235}U and 4.8% ^{235}U cases. However, the core power level is not kept at full power for the entirety of its lifetime. The capacity factor used in the burnup equation is the ratio of the core

lifetime at which the thermal output of the core is at full continuous power output. Earlier in the analysis for the purpose of scoping the required core loading, the capacity factor was assumed to be 1; full power for the entire four year lifetime. In actuality, this ratio is approximately 0.9 for most commercial reactors. For the desired core lifetime a capacity factor of 0.9 translates to 1314days of full power operation. Thus the 5% ^{235}U and 4.8% ^{235}U cases with 4.4% SE remain viable.

4.3. Effect of Burnable Absorber Rods

Burnable Absorber Rods (BARs) are rods that are inserted into the fuel assembly to help control reactivity, minimize power peaking and maximize fuel utilization allowing higher fuel burnup by facilitating uniformity in fuel depletion. Another important function of the BARs is to reduce the initial excess reactivity of the fresh core. This is important since at the initial core loading, the core is more difficult to control. BARs are typically made of material with very large neutron absorption cross-section such as boron carbide, indium-silver-cadmium compounds and gadolinium oxide. Figure 14 shows a BAR loading scheme for a typical PWR with the numbers indicating the number of rods in that assembly location.

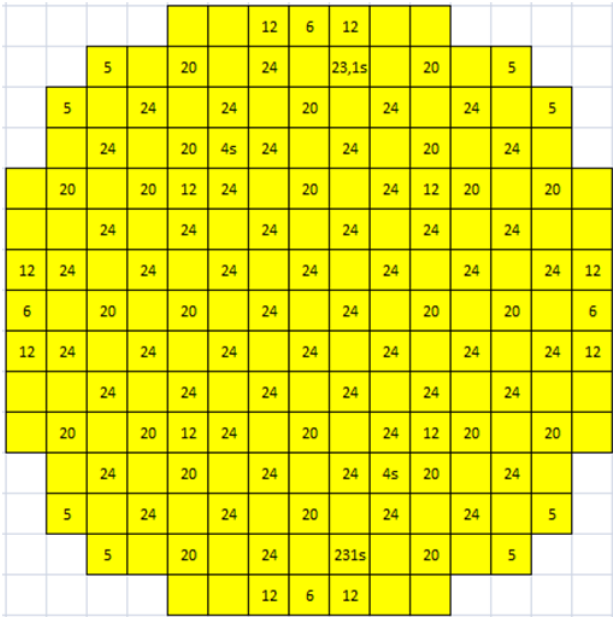

Figure 14: BAR Loading Pattern of a Typical PWR

An ‘s’ denotes a source rod. The same checked scheme was employed in the SMR with natural boron carbide as the neutron absorbing material. The BARs introduced parasitic absorptions but the effect on the core lifetime was found to be limited. The ^{10}B content of the BARs is depleted in the early portion of the core's four year lifetime. As this happens the excess reactivity depressed in the early stages of life is in effect "released" back into the core. The results are presented in Table 7.

For all three test cases, we see from Table 7 that a dramatic decrease in the beginning of life (BOL) effective neutron multiplication factor, from 1.37 to 1.26. This is a significant gain. By having lower excess reactivity at BOL, less control rod worth is required to control the reactor thus there is an overall increase in the safety margins of the reactor.

For the core with no SE assemblies and the core with 5 SE assemblies, the addition of the BARs results in a loss of 90days in core lifetime (See Figure 15 and Figure 16). The 9 SE assemblies cases showed the same behavior resulting in a larger loss in core lifetime of 180days (See Figure 17).

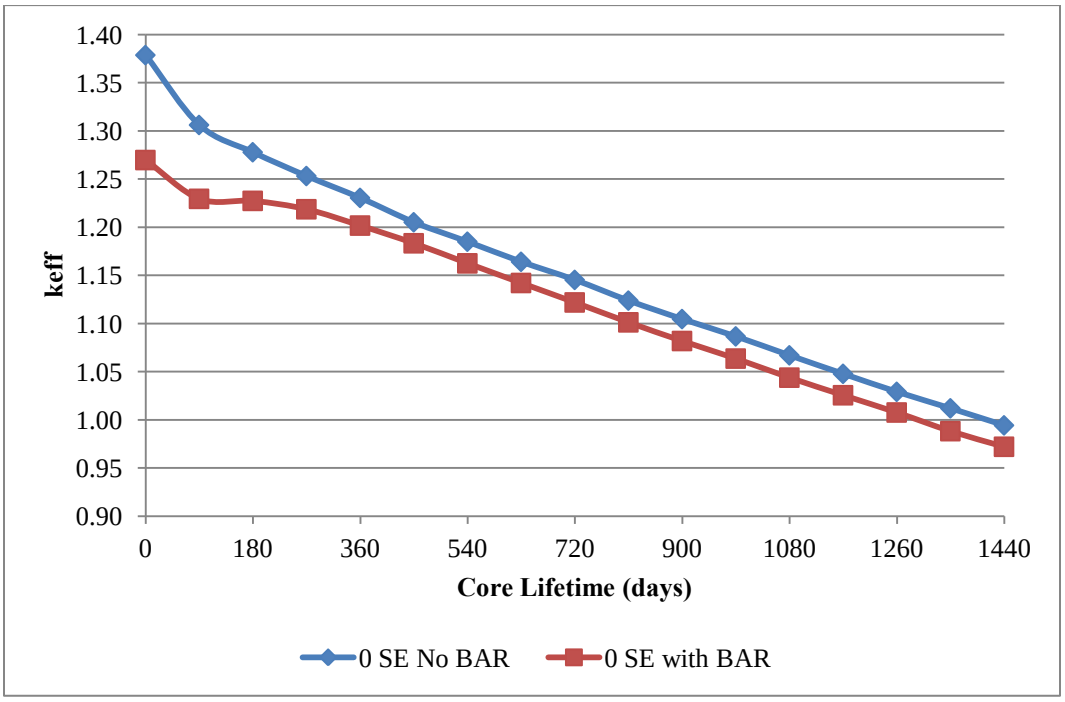

Figure 15: Core Lifetime for Core with No SE Assemblies

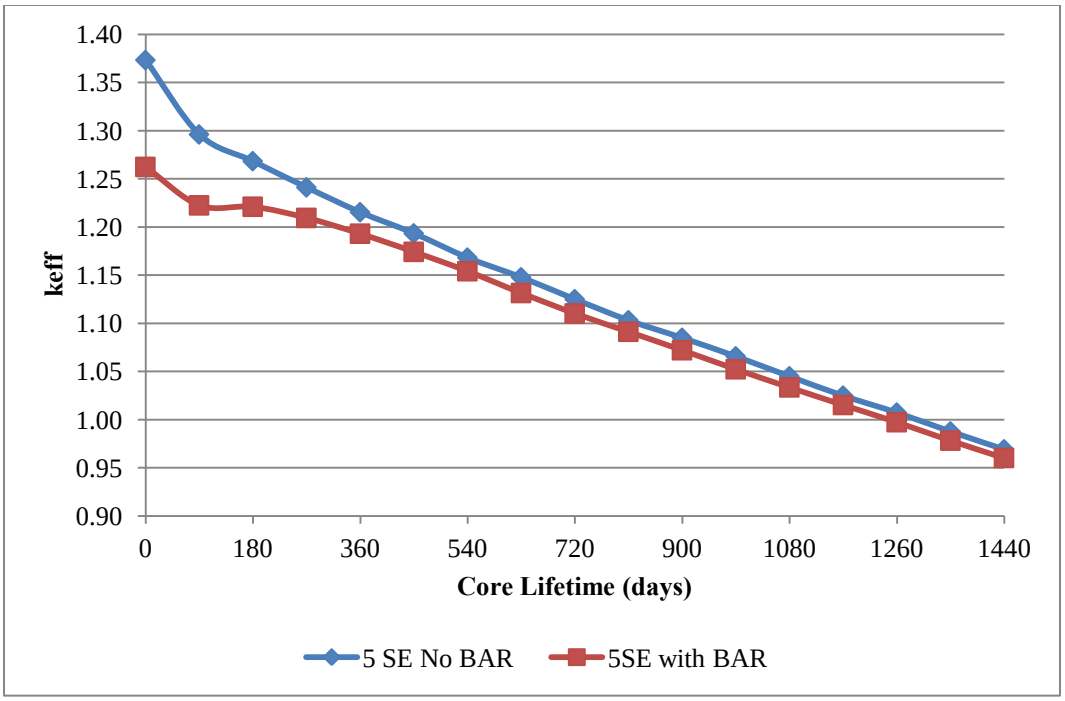

Figure 16: Core Lifetime for Core with 5 SE Assemblies

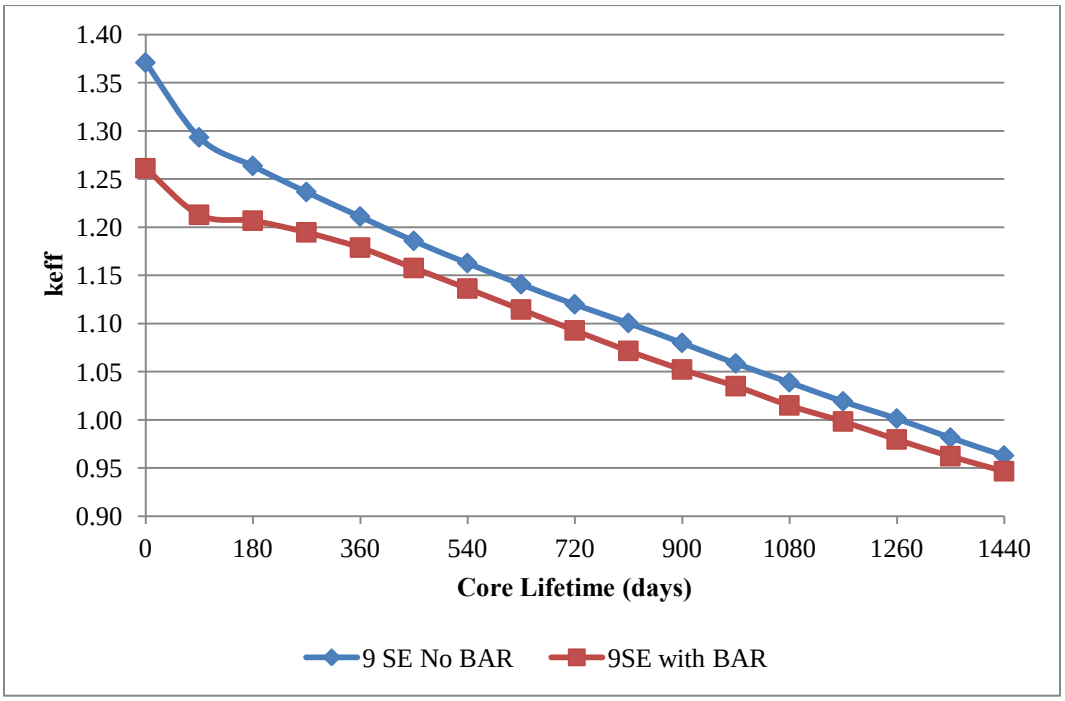

Figure 17: Core Lifetime for Core with 9 SE Assemblies

Table 7: Effect of BAR Loading on Core Lifetime

Time (days)	0 SE Assemblies with BAR	5 SE Assemblies with BAR	9 SE Assemblies with BAR
0	1.26958	1.26233	1.26103
90	1.22931	1.22243	1.21274
180	1.2272	1.22099	1.20664
270	1.21851	1.2094	1.1945
360	1.20156	1.19299	1.17867
450	1.18319	1.17416	1.1575
540	1.16234	1.15404	1.13617
630	1.14195	1.13141	1.11439
720	1.12173	1.11019	1.09268
810	1.10109	1.09118	1.07144
900	1.08169	1.07203	1.05212
990	1.06345	1.05226	1.03479
1080	1.04365	1.03342	1.01479
1170	1.02538	1.01516	0.99813
1260	1.00746	0.9973	0.97946
1350	0.98811	0.97819	0.96207
1440	0.9719	0.96013	0.94645

4.4. Loading Pattern

Thus, the effect of adding SE assemblies and BARs has been investigated. The results of the analysis were used to design viable core loading patterns considering average enrichment, number and position of SE assemblies and number and position of BAR to be used. Several such cores were designed, modeled and analyzed.

It was determined through the depletion calculations, that the 9 SE-assemblies case caused an unacceptable loss in core lifetime. Peaking occurred within the SE assemblies at the centre of the core necessitating the use of BARs in these assemblies. The effect of lower enrichment and burnable absorbers at the centre of the core resulted in a severe loss of reactivity. As such this configuration was discarded in favor of the 5 SE-assemblies case. This is the case that gives reasonable peaking control without suffering significant losses in core lifetime.

In reality, an enrichment of 5%^{235}U is not used as this surpasses the definition of LEU. For safety and licensing considerations, the enrichment is always kept below 5% ^{235}U. In order to arrive at a realistic SMR design, a PE of 4.95% ^{235}U is used in the optimized core.

The 5 SE-assemblies case was further optimized by determining the number and position of BARs necessary to achieve the four-year core lifetime target and the reduced power peaking characteristic required for inherently safe operation. From the results shown in section 4.3, it is clear that the checkered pattern employed in existing large PWRs is effective at minimizing peaking. But superimposing this scheme on the SMR core without modification was inadequate. The optimized core was obtained by starting with a model having a core with all 69 assemblies enriched at 4.95% ^{235}U without BARs. The power peaking factor was calculated by obtaining both the radial and axial power distribution for the core. Based on where peaking occurred, the central 5 assemblies were replaced with secondary enrichment at 4.4%. Again the power peaking is calculated and further modifications made to improve peaking by placing 24, 20 or 12 BARs in the assemblies where peaking occurred.

Figure 18 shows the evolution of the core layout by utilizing BAR number and placement to flatten the core power distribution. The numbers represent the number of BARs in that assembly location. Figure 19 shows the evolution of the core radial power profile as a

result of the optimization. It is clear from these figures that the BARs are having the desired effect of removing the peak and flattening the power distribution within the core.

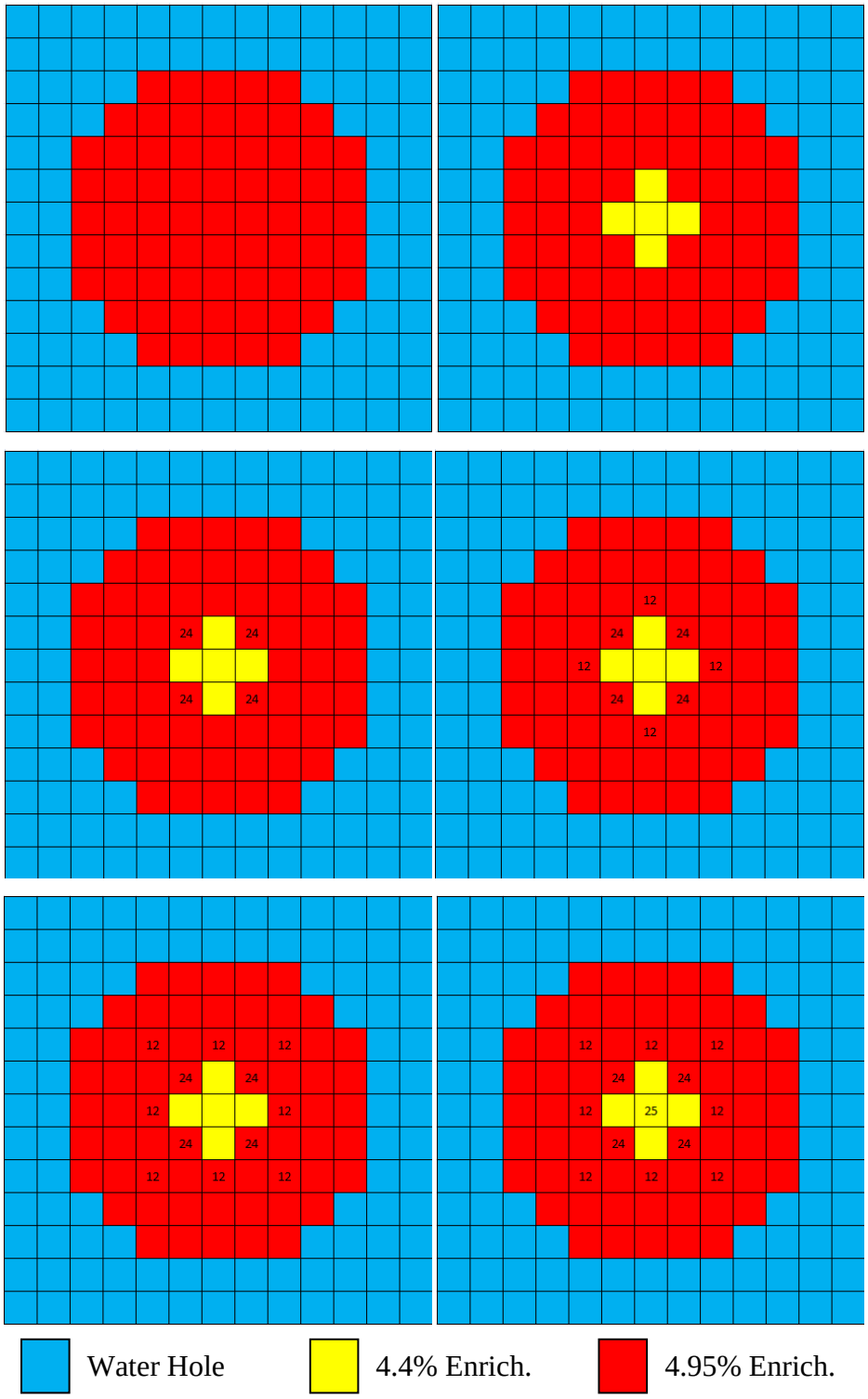

Figure 18: Evolution of SMR Core and No. of BARs

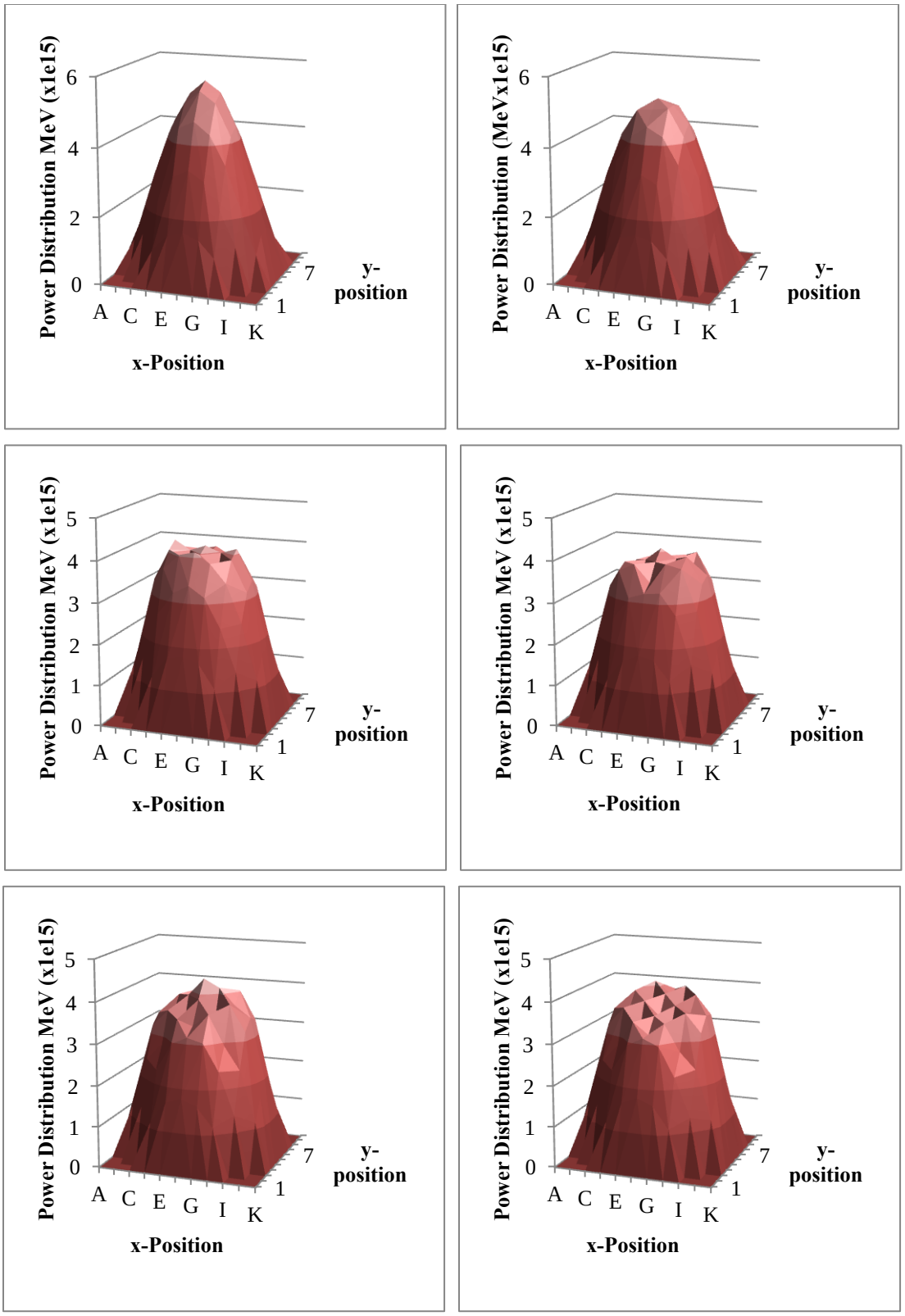

Figure 19: Evolution of the Core Radial Power Distribution

The BAR loading patterns showing favorable peaking behavior were chosen for further analysis. Details for two of such core configurations are presented in Table 8 as Core1 and Core2 respectively.

Table 8: Characteristics of Two Viable Core Loading Patterns

Core Parameter	Core1	Core2
No. of 4.95% enrichment assemblies	64	64
Mass of 4.95% enriched Fuel (tons)	17.0788	17.0788
No. of 4.4% enrichment assemblies	5	5
Mass of 4.4% enriched Fuel (tons)	1.33428	1.33428
Total Fuel Mass (tons)	18.41308	18.41308
Average enrichment (%)	4.91	4.91
No. of BARs	96	216
Mass of BAR material (kg)	8005.435	11341.034
Achieved Core Lifetime	1230	1230
Average Fuel Burnup (GWD/MTU)	38.81	38.81
Effective Multiplication Factor at EOL	1.00153	1.00133

4.5. Neutron Flux and Power Distributions

The neutron flux and power distributions within the core are very important parameters to know about the reactor core. They are vital to both neutronics and thermal hydraulics; affecting reactor behavior and heat removal considerations. For neutronics, the locations of the peaks in the neutron flux distribution indicate the optimum locations for

control rods in order to control the reactor. For thermal hydraulics, the peak power locations are where peak temperatures occur which could lead to localized boiling, and fuel/clad melting; all undesirable phenomena. The two are inextricably linked since the neutron flux drives the fission rate which in turn drives the power production rate.

$$Fission\ Rate\ Density = \phi \sum_f$$

$$Power\ Density = \eta \varepsilon_f \phi \sum_f$$

where ϕ is the neutron scalar flux, $\sum_f$ is the total macroscopic fission cross section, ε_f is the energy produced per fission and η is a ratio of total energy produced by fission to total energy. η is important because although a majority of the thermal energy produced comes from fission, there is also gamma heating present in the core from the photon interactions. Using the neutron and photon energy deposition tally feature in MCNP, total energy deposited per unit volume per second (Power Density) was obtained.

4.5.1. Power Peaking Factor

Now that the flux and power distributions are defined, the radial and axial power peaking factors can be obtained using these definitions. The radial peaking factor is the ratio of the average power in the hottest assembly in the core, to the average power of the entire core. Likewise, the axial peaking factor is the ratio of the power in the hottest axial zone of the hottest assembly to the average power of all the axial zones of the hottest assembly. Peaking factors are used to determine expected characteristics of hotspots given that the core average parameters are known. The total power peaking factor is the product of the radial and axial peaking factors.

$$Radial\ Peaking\ Factor\ \left(F_r^p\right) = \frac{Maximum\ Radial\ Power}{Average\ Radial\ Power}$$

$$Axial\ Peaking\ Factor\ \left(F_z^p\right) = \frac{Maximum\ Axial\ Power}{Average\ Axial\ Power}$$

$$Total\ Peaking\ Factor\ \left(F_{tot}^{p}\right) = F_{r}^{p} \times F_{z}^{p}$$

The radial, axial and total power peaking factors were found for both cores and are presented in Table 9.

Table 9: Power Peaking Factors for Core Loading Patterns Core1 and Core2

		Average Power per Assembly (MeV/s)	Peak Assembly Power (MeV/s)	Peaking Factor	Total Peaking Factor
Core1	**Radial F_r^p**	3.29E+15	4.07E+15	1.24	1.35
	Axial F_z^p	4.43E+15	4.84E+15	1.09	
Core2	**Radial F_r^p**	3.23E+15	3.89E+15	1.20	1.49
	Axial F_z^p	3.70E+15	4.58E+15	1.24	

The lower value of the total power peaking factor of Core1, indicates that this core loading pattern can be expected to produce a more inherently safe reactor with lower peak temperatures and reduced chance of temperature driven transients leading to eventual fuel and/or clad damage. Additionally, a lesser number of BARs are required in this configuration. This is a positive from an economic standpoint in reduced cost. As a result, Core2 was discarded and Core1 kept as the optimized SMR design. Figure 20 and Figure 21 show the Power Distribution for the optimized core. Figure 22 and shows the Axial Power Distribution for the optimized core

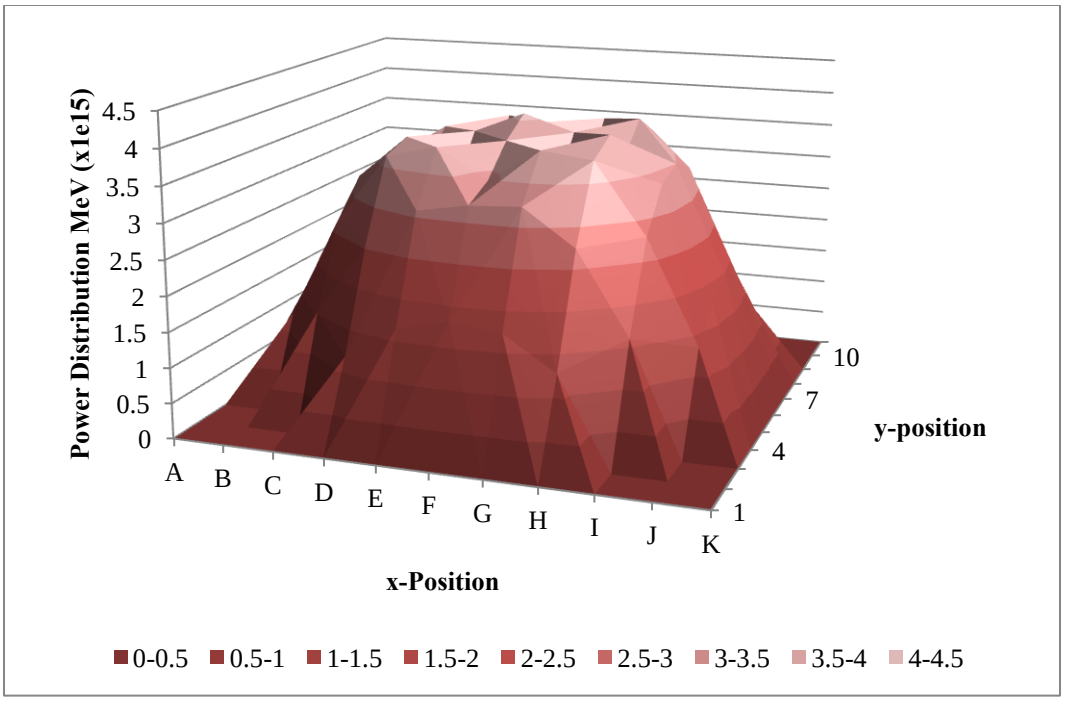

Figure 20: 3D View of the Power Distribution for Optimized Core

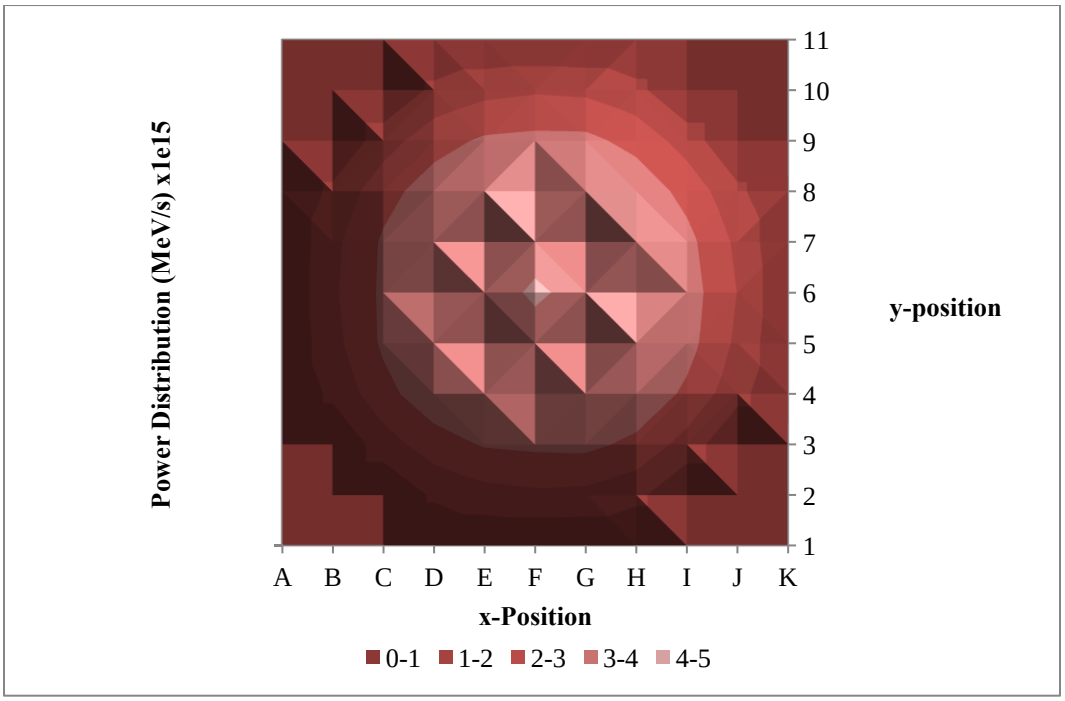

Figure 21: Plan View of the Power Distribution for Optimized Core

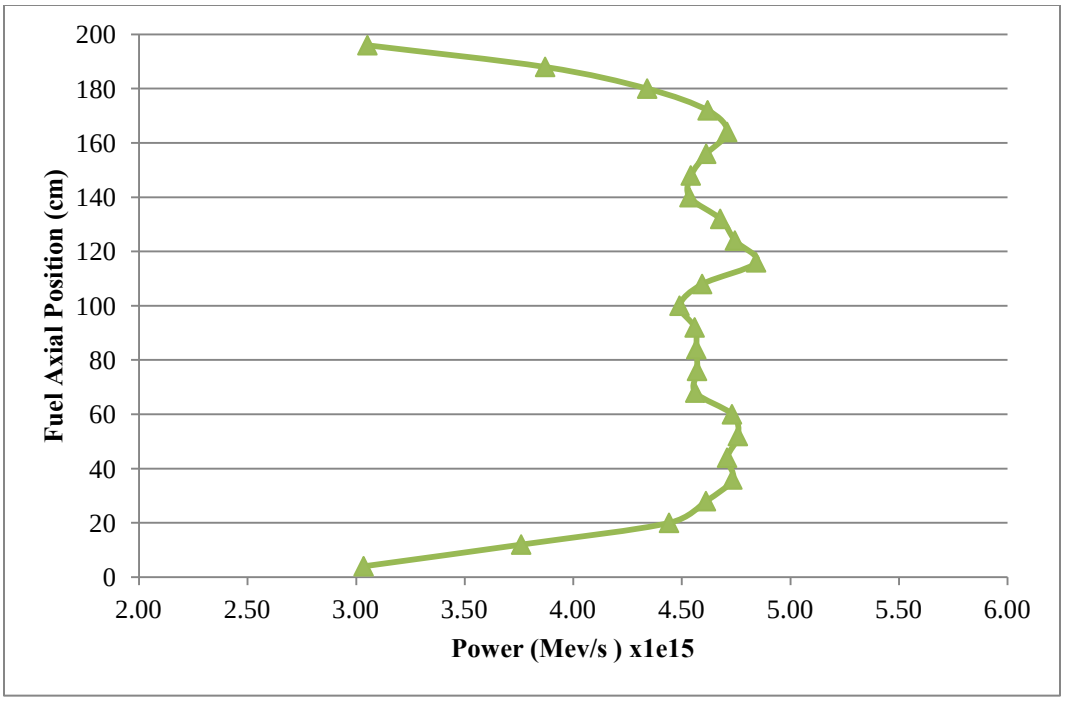

Figure 22: Axial Power Distribution for Hottest Assembly in Core1

4.6. Optimized Core Lifetime and Fuel Burnup

4.6.1. Optimized Core Lifetime

The optimized core has an active fuel length of 200cm for an H/D ratio of 1.028. Fuel enrichment levels were set at 4.95% and 4.4% ^{235}U for the primary and secondary enrichments. The core comprised of 69 fuel assemblies and the loading pattern of the BARs is optimized to reduce peaking while maximizing fuel utilization. Table 10 shows the optimized core parameters.

With the SMR model finalized, a more detailed depletion calculation is required to determine more accurately the core lifetime and the level of burnup reached by the fuel. In order to do so, each fuel pin is divided axially into 10 regions and defined as a separate material in MCNP. Thus the number materials burned increased from 3 materials (2 fuel materials and 1 BAR material) to 21 materials (20 fuel materials and 1 BAR material). This increases the accuracy of the calculation since each section of the fuel is treated with its

position dependant flux instead of the flux being averaged over the entire pin. Smaller burn steps were added at the BOL to accurately determine the equilibrium concentrations of fission products which lower core reactivity. Smaller burn steps were also added at EOL to accurately determine the EOL fuel isotopic composition and core lifetime.

The results showed a lower value for the effective multiplication factor at each step. This did not result in a reduction in the predicted core lifetime but rather an increase of twenty additional days. Table 11 shows behavior of the effective multiplication factor for the optimized core over its lifetime and the core average burnup. The data is presented in Figure 23.

Table 10: Optimized Core Parameters

Parameter	Value
Active Fuel Length (cm)	200
Height-to-diameter ratio	1.028
Fuel Enrichment	Primary - 4.95% 235U. Secondary 4.4% 235U
Core Size	69 Fuel Assemblies
Fuel Loading Pattern	Optimized – 64 Primary, 5 Secondary
Total Fuel Mass (tons)	18.41308
Bar Loading Pattern	Optimized
Number of BARs	96
Mass of BAR material (kg)	8005.435
Achieved Core Lifetime	1230
Average Fuel Burnup (GWD/MTU)	38.81
Radial and Axial Peaking Factors	1.24 and 1.09
Total Peaking Factor	1.45

Table 11: Effective Multiplication Factor (k_{eff}) over Optimized Core Lifetime

Time (days)	Effective Multiplication Factor	Core Average Burnup	Time (days)	Effective Multiplication Factor	Core Average Burnup
0	1.3534	0.00	**720**	1.13161	22.18
0.3	1.34231	0.01	**810**	1.10924	25.00
0.6	1.29750	0.02	**900**	1.08713	27.81
1	1.32048	0.03	**990**	1.06599	30.63
2	1.31466	0.06	**1080**	1.04493	33.45
30	1.30167	0.92	**1170**	1.02291	36.26
90	1.29080	2.77	**1190**	1.01764	36.89
180	1.27310	5.55	**1210**	1.01136	37.51
270	1.25147	8.32	**1230**	1.00719	38.14
360	1.22741	11.09	**1250**	1.00317	38.77
450	1.20348	13.87	**1270**	0.99903	39.39
540	1.18052	16.64	**1290**	0.99373	40.02
630	1.15891	19.41	**1310**	0.98955	20.64

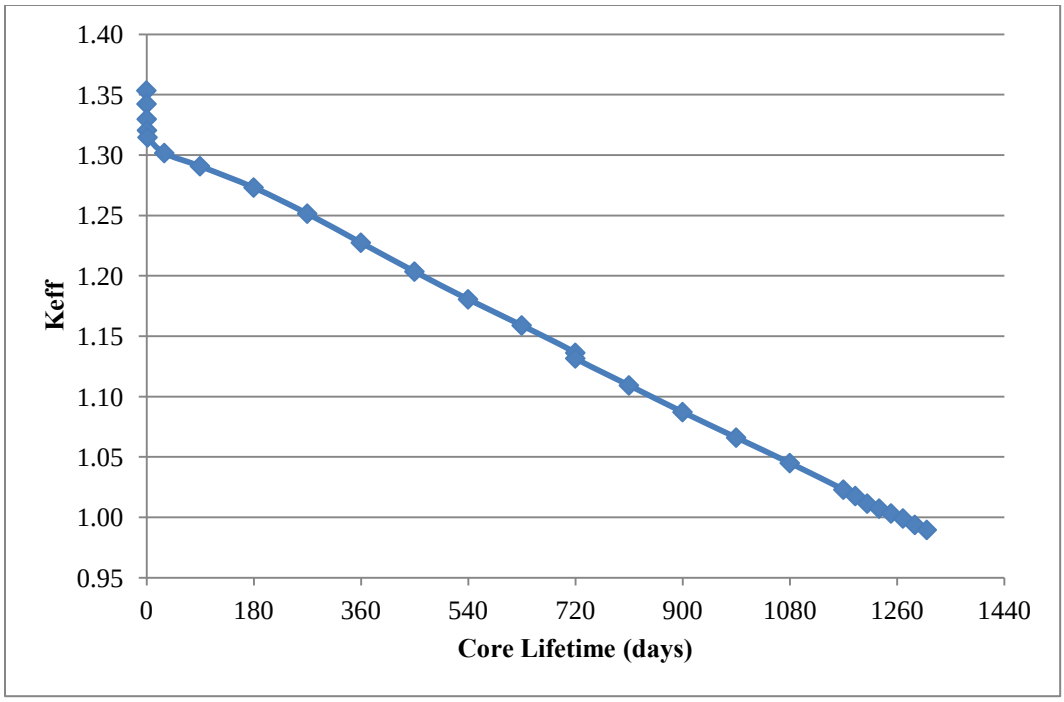

Figure 23: Effective Multiplication Factor for Optimized Core over Core Lifetime

The core is found to reach a 1250days of full power operation with k_{eff} = 1.00317 at this last point above criticality. Methods exist in the operation of nuclear reactors to extend the core lifetime by changing other plant parameters. Actions such as decreasing the inlet coolant temperature or dropping the depleted BARs out of the core all serve to increase reactivity. It is conceivable that the SMR will have equivalent measures by which the core lifetime can be extended by as much as 50days. Claiming a core lifetime of 1270days based on the above data is still a conservative result.

4.6.2. End of Life Isotopic Composition

The EOL isotopic composition is important for a variety of reasons. The most important of these from a proliferation resistance point of view is the plutonium content of the spent fuel. Table 12 shows the average gram quantities and activities of a few important isotopes in a PE spent fuel assembly.

Table 12: EOL Isotopic Composition for a PE Spent Fuel Assembly

Element	Isotope	Mass (g)	Activity (Ci)
Uranium (U)	233	1.764E-04	1.700E-06
	234	6.792E-01	4.223E-03
	235	3.791E+03	8.192E-03
	236	1.346E+03	8.706E-02
	237	1.956E+00	1.597E+05
	238	2.203E+05	7.405E-02
	239	1.043E-01	3.494E+06
Plutonium (Pu)	238	3.048E+01	5.219E+02
	239	1.244E+03	7.714E+01
	240	4.694E+02	1.065E+02
	241	2.800E+02	2.894E+04
	242	8.739E+01	3.456E-01
	243	1.842E-02	4.792E+04
	244	1.892E-03	3.466E-08
Cesium (Cs)	133	2.963E+02	0.000E+00
	134	2.970E+01	3.845E+04
	135	1.257E+02	1.448E-01
	136	1.522E-01	1.111E+04
	137	3.198E+02	2.784E+04
Europium (Eu)	151	2.983E-03	0.000E+00
	152	3.583E-03	6.325E-01
	153	2.534E+01	0.000E+00
	154	5.602E+00	1.514E+03
	155	1.823E+00	8.988E+02

4.7. Reactor Kinetics Parameters

The Point Reactor Kinetics Equations (PRKEs) are a coupled set of equations for the neutron balance in a system. They allow for a simple treatment of the time dependence of chain reaction by making assumptions to eliminate the spatial and energy dependence in the neutron transport equation leaving time as the only variable. The parameters in these equations are commonly referred to as the reactor kinetics parameters.

A common form of the PRKEs assuming one energy group and no external source is:

$$\frac{d}{dt}n(t) = \frac{\rho - \beta}{\Lambda}n(t) + \lambda C(t)$$

$$\frac{d}{dt}C(t) = \frac{\beta}{\Lambda}n(t) - \lambda C(t)$$

where $n(t)$ is the neutron population, ρ is the reactivity, β is the delayed neutron fraction, Λ is the prompt generation time, λ is the decay constant of the delayed neutron precursors and $C(t)$ is the delayed neutron precursor population.

4.7.1. Delayed Neutron Fraction

Not all neutrons produced from fission are released instantaneously at the time of fission. Some neutrons are released at a later time as they are a product of the decay chain of the resulting fission products. These delayed neutrons play a key role in determining the ease with which the chain reaction can be controlled. The delayed neutron fraction is a ratio of the number of neutrons that are delayed to the total number or neutrons produced from fission. A large delayed neutron fraction results in a relatively slower rate of change in the neutron population and a relatively easier to control reactor.

The effective multiplication factor is calculated for the model with and without the contribution from delayed neutrons using the TOTNU card in MCNP5.

The delayed neutron fraction is calculated as

$$\beta_{eff} = \frac{k_{eff} - k_p}{k_{eff}}$$

where β_{eff} is the delayed neutron fraction, k_{eff} is the effective neutron multiplication factor and k_p is the neutron multiplication factor with only prompt neutrons.

Figure 24 shows the delayed neutron fraction for the optimized core calculated over its lifetime. Thus the effective delayed neutron fraction starts at 0.00640. This is typical of LEU systems (Muhammad, 2010) and decreases steadily to 0.00448 at EOL. This is primarily due to the build-up of plutonium in the core. Plutonium has a lower delayed neutron fraction than ^{235}U. This translates to an increasingly difficult reactor to control. However this is not a cause for concern as the excess reactivity is decreasing as the core is depleted and any reactivity induced transients will be diminished in magnitude.

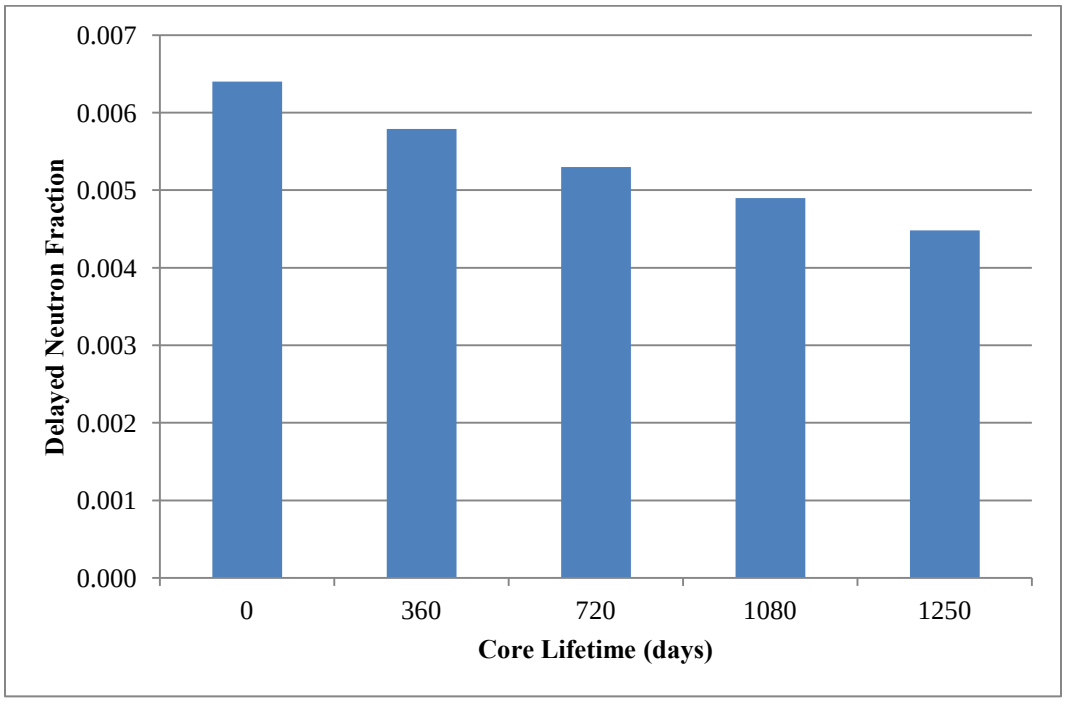

Figure 24: Effective Delayed Neutron Fraction for Optimized Core

4.7.2. Mean Generation Time

A neutron in the reactor can have a number of interactions within the core before leaking out of the core or being absorbed. If the absorption leads to fission, the neutrons resulting from this fission are said to be the next generation of neutrons. The mean generation time is the average time it takes for one neutron to produce another through fission. Along with the delayed neutron fraction, the mean generation time is a good indicator of the relative difficulty in control a system will pose. The mean generation time is calculated as

$$\Lambda = \frac{l_p}{k_{eff}}$$

where Λ is the mean generation time, k_{eff} is the effective neutron multiplication factor and l_p is the prompt neutron lifetime. l_p is the average time for a prompt neutron to be removed from the system by leakage or absorption. Figure 25 and Figure 26 show the mean generation time and excess reactivity for the optimized core over its lifetime. Notice the decrease in core excess reactivity with time as the core is depleted.

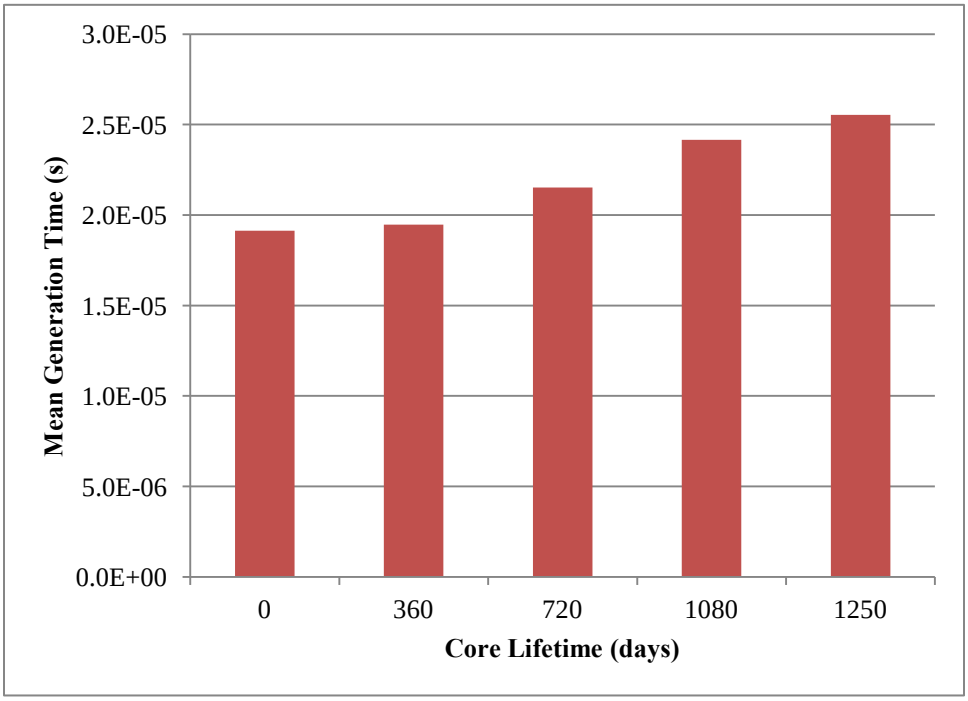

Figure 25: Mean Generation Time for Optimized Core

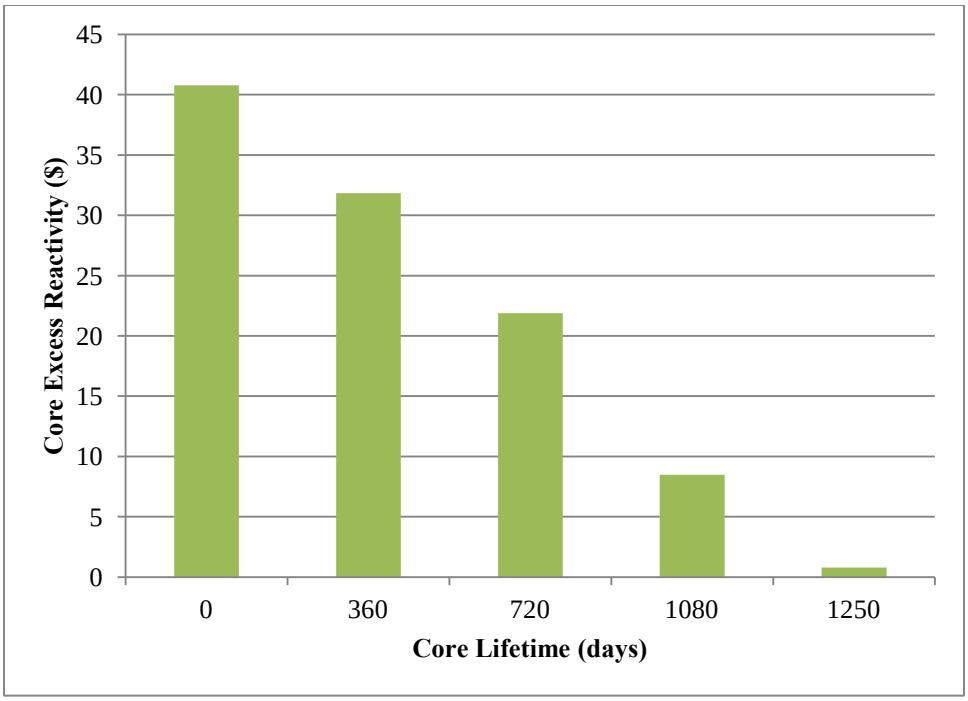

Figure 26: Excess Reactivity for Optimized Core

Table 13 presents a summary of the reactor kinetics parameters for the optimized core

Table 13: Reactor Kinetics Parameters for Optimized Core

Time (days)	Effective Multiplication Factor k_{eff}	Prompt Multiplication Factor k_p	Mean Generation Time (s) Λ
0	1.35309	1.34509	1.91E-05
360	1.22602	1.21832	1.95E-05
720	1.13114	1.12622	2.15E-05
1080	1.04345	1.03936	2.42E-05
1250	1.00357	0.99730	2.55E-05

Table 13 Continued: Reactor Kinetics Parameters for Optimized Core

Time (days)	Effective Delayed Neutron Fraction β_{eff}	Excess Reactivity ($) $\rho = \frac{k_{eff} - 1}{k_{eff}} \times \frac{1}{\beta_{eff}}$
0	0.00640	40.77
360	0.00579	31.84
720	0.00530	21.87
1080	0.00490	8.50
1250	0.00448	0.79

4.8. Reactivity Coefficients

The withdrawal of a control rod from the reactor core leads to an increase in reactivity and the fission rate within the fuel elements. This subsequently results in a greater thermal energy output. Along with this power increase is an increase in the fuel temperature. At higher temperatures however, the effective absorption cross section of the fissile material is decreased (Doppler broadening) leading to negative reactivity feedback and decrease in the fission rate and power level. The reactivity coefficients help to quantify the magnitude of the feedback effects and are a quantitative indicator of how a change in one core parameter such as fuel temperature or power level affects the reactivity of the core. For a change in a parameter$x$, from x_1 tox_2, the reactivity coefficients are defined as

$$\alpha_x = \frac{\Delta\rho}{\Delta x} = \frac{\rho_2 - \rho_1}{x_2 - x_2}$$

where α_x is the reactivity coefficient for a change in parameter$x$, Δx is the change in parameter x and $\Delta\rho$ is the accompanying change in reactivity.

For inherently safe operations, it is desirable to have all the major reactivity coefficients be negative. Negative coefficients ensure that there are no scenarios in which an increase/decrease in one parameter causes a reactivity change which causes the parameter increase/decrease again thus entering a never ending loop. Negative coefficients ensure negative feedback; for example an increase in power leads to changes that cause power to decrease. Thus any transients will be self limiting before material and other physical constraints such as fuel melting are reached.

Of the reactivity coefficients, the fuel temperature coefficient of reactivity also known as the Doppler coefficient is the most important. The Doppler coefficient reflects the change in reactivity caused by Doppler Broadening of the neutron cross-section for the uranium fuel material as a result in a change in temperature of the material. This coefficient must be negative for an inherently safe reactor design. This is because temperature changes in the fuel occur on a very short time scale in the order of microseconds compared to that of other changes in the order of seconds to minutes. Hence Doppler feedback tends to dominate the other feedback effects.

The moderator temperature coefficient of reactivity is another important reactivity coefficient. This reflects the change in reactivity due to a change in the moderator temperature. Since the coolant/moderator for the SMR design is light water, there are also density changes associated with the change in temperature that have to be accounted for. Increasing moderator temperature in the case of water results in a decrease in absorptions in the water which is a positive feedback effect. However, the density is simultaneously decreasing and results in reduced moderating capability which for a thermal reactor results in negative feedback. Thus the moderator coefficient for the SMR will reflect the relative strength of these competing phenomena.

The void coefficient of reactivity reflects the change in reactivity as a result in the change percent void in the coolant channel. Voiding can occur for a variety of reasons; boiling of the coolant and a break in the coolant pipe. As most coolant pipes have been eliminated in the SMR by pursuing the IPWR configuration, boiling remains the most likely cause of voiding in the reactor. Localized boiling most likely occurs at hotspots on the surface of the clad. This will lead to a dramatic reduction in the moderation available thereby reducing the fission rate and hence the temperature and reducing the boiling.

The power coefficient of reactivity is the sum of all the reactivity effects resulting from a change in core power level. This includes the fuel temperature, moderator temperature and sometimes voiding. The power coefficient of reactivity must remain negative for the entire lifetime of the core for inherently safe operation of the SMR.

The reactivity coefficients were calculated for optimized model of the SMR over its lifetime and are presented in Table 14 and Figure 27. From the results, it is clear that all coefficients are negative for the entirety of the core lifetime. This is important for inherently safe operations. The coefficients become increasingly negative as the core evolves with the most negative value at EOL.

Table 14: Reactivity Coefficients for Optimized Core

Time (days)	**Doppler** $\frac{\Delta k}{k}/_{°K}$	**Moderator Temp.** $\frac{\Delta k}{k}/_{°K}$	**Void** $\frac{\Delta k}{k}/_{\%void}$	**Power** $\frac{\Delta k}{k}/_{\%Power}$
0	-0.000014	-0.000123	-0.001326	-0.000412
360	-0.000022	-0.000134	-0.001687	-0.000468
720	-0.000019	-0.000163	-0.001875	-0.000545
1080	-0.000021	-0.000194	-0.002117	-0.000644
1250	-0.000027	-0.000204	-0.002504	-0.000694

As mentioned earlier, although the Doppler coefficient seems to be the smallest, it is the most important as it operates on a very short timescales. The moderator temperature coefficient clearly shows that the loss of moderation due to the reduced density accompanying a moderator temperature increase dominates any gains from reduced absorptions in the coolant/moderator.

Similar to the moderator coefficient case, we see that the void coefficient is very large and negative. Introducing a void in the coolant/moderator reduces moderation and in a thermal reactor, this causes a decrease in reactivity.

The power coefficient as expected follows the Doppler and Moderator coefficients and remains negative for the entire core lifetime.

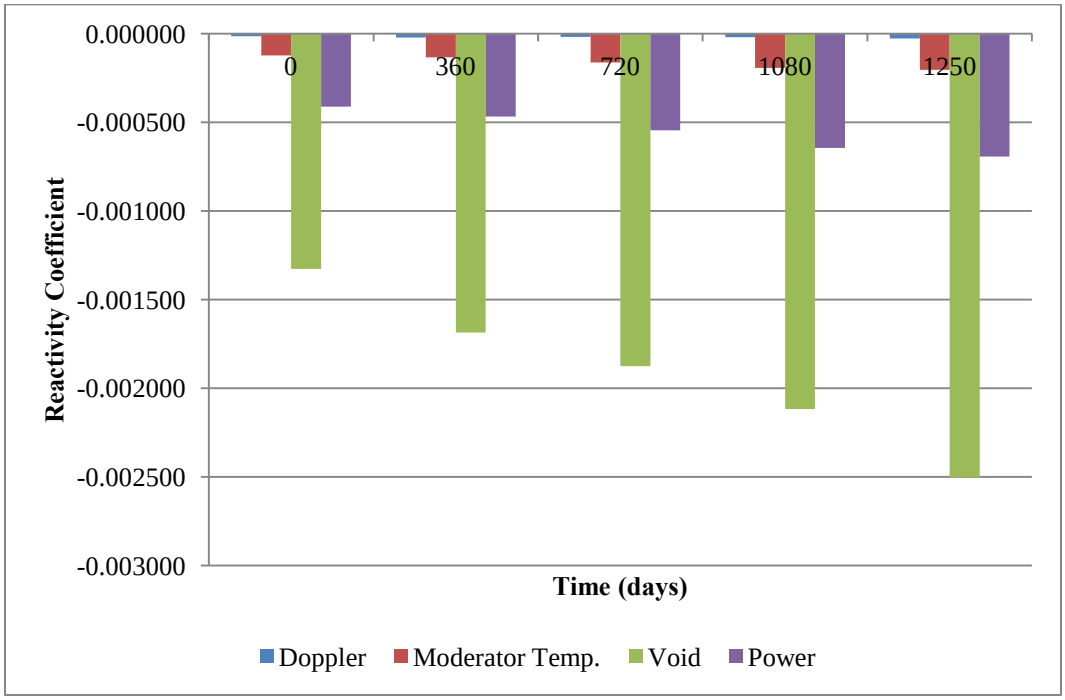

Figure 27: Reactivity Coefficients for Optimized Core

4.9. Newest mPower Information

To this point the neutronics assessment of the SMR is complete. The analysis and optimization of the design has resulted in a core producing an energy output of 500MWth for 1270 days continual operation at full power equating to a capacity factor of 0.87. This however falls short of the 4year (1460) goal set for the design and the assumed capacity factor of 0.9. The average fuel burnup achieved is 38.77GWd/MTU also short of the targeted 40GWd/MTU.

Through the development of the model, it has been clearly shown that the targeted 4year core lifetime producing produce 500MW of thermal energy output and 40GWd/MTU fuel burnup cannot be attained with this configuration. Increasing fuel enrichment is not viable, as at 4.95% ^{235}U, the upper limit of 5% ^{235}U has been effectively reached. The only remaining avenue withstanding further optimization is to increase the active fuel length above the stated 200cm. The findings of the height-to-diameter analysis showed that the active fuel length can be increased substantially (by up to 50cm) and a neutronically favorable configuration still attained.

Recent information released by mPower (June 2012) regarding the SMR currently under development confirm these findings. The new information describes an mPower SMR with an active fuel length of 95in (~240cm) and rated at 530MWth (Babcock & Wilcox, 2012). In light of this new information, depletion calculations were executed to determine whether the original targets are attained under these new design parameters. This was done to as a confirmation of the results of the current work and optimization of this new configuration was not done. Indeed the results of the depletion calculations (Table 15 and Figure 28) revealed that the four year core lifetime is easily achievable with the increased fuel length and power.

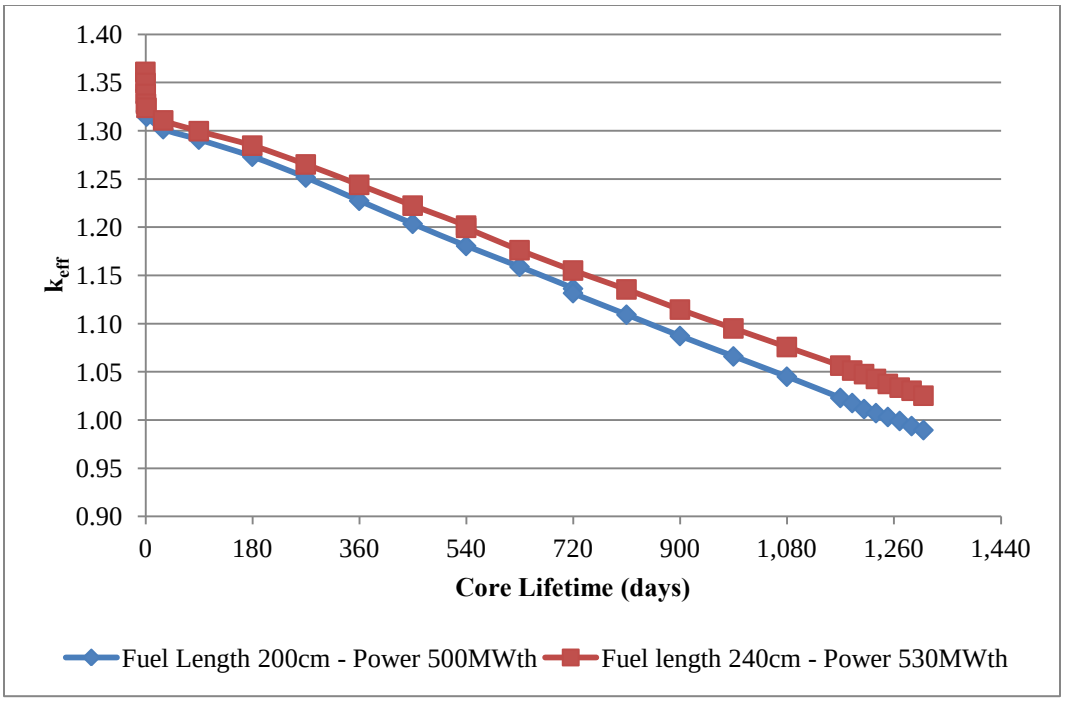

Figure 28: Comparison of the Effective Multiplication Factor

Table 15: Effective Multiplication Factor with New mPower Information

Time (days)	Effective Multiplication Factor	Core Average Burnup	Time (days)	Effective Multiplication Factor	Core Average Burnup
0	1.36105	0.00	**720**	1.15505	19.65
0.3	1.34947	0.01	**810**	1.13545	22.125
0.6	1.33817	0.02	**900**	1.11458	24.60
1	1.32802	0.03	**990**	1.09498	27.07
2	1.32377	0.05	**1080**	1.07570	29.55
30	1.31074	0.82	**1170**	1.50643	32.02
90	1.29958	2.45	**1190**	1.05133	32.57
180	1.28456	4.90	**1210**	1.04761	33.12
270	1.26507	7.35	**1230**	1.04260	33.67
360	1.24390	9.798	**1250**	1.03744	34.22
450	1.22234	12.25	**1270**	1.03358	34.77
540	1.19932	14.70	**1290**	1.03039	35.32
630	1.17617	17.17	**1310**	1.02524	35.87

5. THERMAL HYDRAULICS

Now that the reactor concept has been developed into a model and optimized to demonstrate desirable neutronics characteristics, thermal hydraulics assessment is required to determine if the thermal energy produced in the core can be safely and efficiently removed for the production of electricity.

Thermal Hydraulics is a large field of its own with many advanced methods in determining temperature profiles, coolant velocity profiles and other important characteristics. Performing such a fully fledged assessment with high fidelity on a reactor concept is very tasking and fully involved. The engineering design of a reactor core will require much iteration with optimization based on the interplay of the neutronics and thermal hydraulics characteristics of the design.

The aim of this chapter is not to do such an in-depth assessment. This chapter will use analytical models and equations to demonstrate that the SMR core model that has been developed is also feasible from a thermal hydraulics and heat removal standpoint.

5.1. Single Channel Analysis

Single channel focuses the thermal hydraulics and thermodynamic analysis efforts on a single isolated vertical flow channel. Typically the hottest flow channel is selected as an upper bound on the temperatures, heat fluxes and pressure drops that can be expected in any flow channel within the core. Thus single channel analysis is often also referred to as Hot Channel Analysis. The aim of the analyses is to determine key parameters regarding the heat removal capabilities of the core and more importantly, affirm the safety characteristics of the reactor.

The following sections focus on fuel temperature distributions in the radial and axial directions and also the critical heat flux and departure from nucleate boiling ratio (DNBR) for the hottest flow channel.

5.2. Fuel Temperature Distribution

As previously discussed in section 4.8 regarding the Doppler coefficient of reactivity, fuel temperatures heavily affect the rate at which fissions occur and hence directly result in changes in thermal energy output. Temperature variations also cause changes in physical characteristics of the fuel material itself such as density, again affecting heat production rates through fission. Other physical properties that are temperature dependent include the material thermal conductivity which inevitably hugely affect the rate at which heat produced in the fuel is dissipated through the gap and cladding to the coolant.

5.2.1. Radial Fuel Temperature

In the radial direction, the fuel, gap and clad temperature distributions are of interest. In order to determine the radial temperature distribution within the fuel element, the maximum temperature within the fuel element must be found. This can be done by assuming that the total core power (Q) is evenly distributed throughout the fuel pins within the core. Then by definition,

$$Core\ Power = Q$$
$$Core\ Power\ Density = Q'''$$
$$Average\ Fuel\ Pin\ Power = q_{FE}$$
$$Average\ Volumetric\ Heat\ Generation\ Rate = q'''_{FE}(r)$$
$$Average\ Surface\ Heat\ Generation\ Rate = q''_{FE}(S)$$
$$Average\ Linear\ Heat\ Generation\ Rate = q'_{FE}(z)$$

The core power is set at 500MWth and the core power density in known from the core power distribution determined using MCNP5. Applying the peaking factors calculated in section 4.5.1, the parameters for the hottest pin in the hottest assembly can be determined. The heat equation can then be solved for the different regions of the fuel element and by applying Fourier's Law of heat conduction, the temperature distribution determined. In order to do this analytically, assumptions must be made.

These assumptions are:

- Thermal conduction is only considered in one dimension. For the radial case, axial heat conduction is neglected
- The fission source appears as uniform heat source distributed throughout the fuel element. $q''' = constant$
- Steady state heat transfer
- Material properties such as thermal conductivities and densities are assumed to be constant for the fuel, gap

The maximum surface heat flux is given by $q''_{FE,max} = F^P_{tot} \times q''_{FE}$ and then the analytical solutions for the radial temperature distributions can be found.

$$T_F(r) = T_{max} - \frac{q'''_F}{4k_F} \times r^2, \qquad 0 \le r \le r_F, \qquad fuel\ region$$

$$T_G(r) = T_{CI} + \frac{q'''_F r^2}{2k_G} \times ln\left(\frac{r_C}{r}\right), \qquad r_F \le r \le r_{CI}, \qquad gap\ region$$

$$T_C(r) = T_{CI} + \frac{T_{CI} - T_{CO}}{ln\left(\frac{r_{CO}}{r_{CI}}\right)} \times ln\left(\frac{r_{CI}}{r}\right), \qquad r_{CI} \le r \le r_{CO}, \qquad clad\ region$$

where$T_F(r)$, $T_G(r)$ and $T_C(r)$ are the temperature distributions in the fuel, gap and clad respectively. T_{max}, T_{CI} and T_{CO} are the temperatures at the centre of the fuel, the inner surface of the clad and the outer surface of the clad respectively. r_F, r_{CI} and r_{CO} are the radii of the fuel region, inner surface of the clad and outer surface of the clad respectively.

The maximum temperature T_{max} can be found by adding the temperature drop over the fuel element ΔT_{FE} to the temperature at the outer surface of the clad T_{CO}which is in contact with the coolant. Using Newton's Law of cooling,$q'' = h(T_{CO} - T_b)$ and a known coolant bulk temperature T_b and heat transfer coefficient$h$, solving for T_{CO} is a trivial task.

$$T_{max} = T_{CO} + \Delta T_C + \Delta T_G + T_F = T_{CO} + \frac{q'}{2\pi f_F} \times \left[\frac{r_F}{2k_F} + \frac{r_{CI} - r_F}{k_G} + \frac{r_{CO} - r_{CI}}{k_C}\right]$$

Figure 29 shows the fuel element radial temperature distribution.

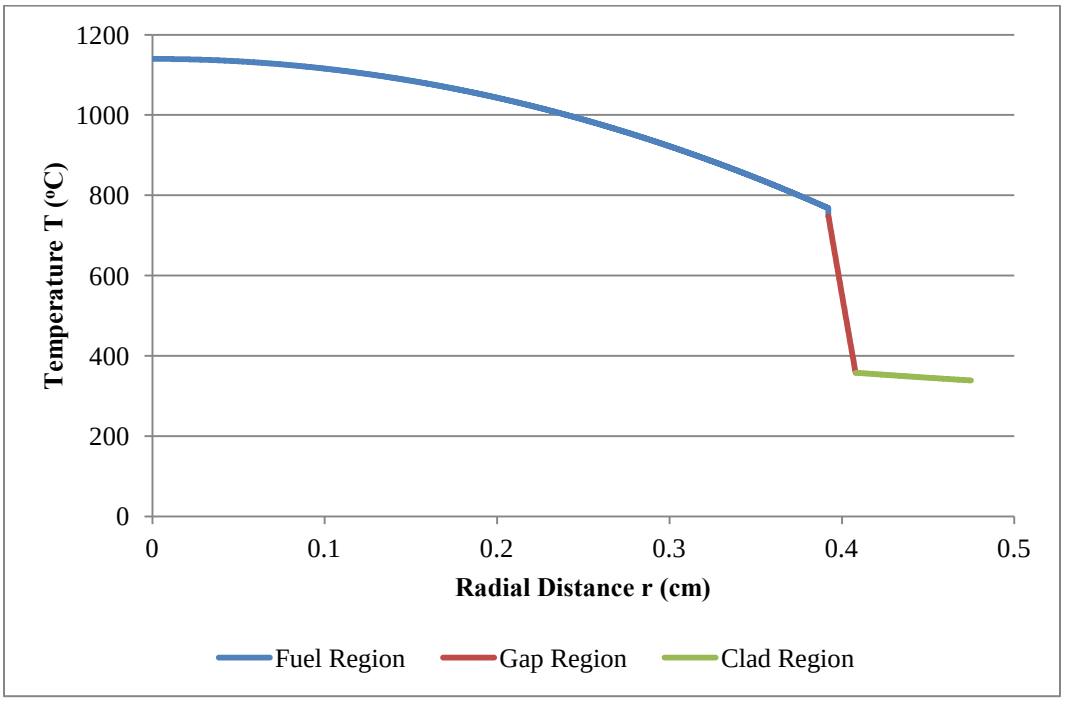

Figure 29: Fuel Element Radial Temperature Distributions

5.2.2. Axial Fuel Temperature

In the axial direction, in addition to the fuel, gap and clad temperature distributions, the bulk coolant temperature distribution is also important. The temperature of the coolant exiting the core and entering the steam generator is extremely important as this drives the secondary side and determines the quality of steam supplied to the turbine and the overall efficiency of the system in generating electricity.

The axial volumetric heat generation rate is highly dependent on the shape of the neutron flux. From nuclear reactor theory, we know that the shape of the neutron flux in the axial direction for a bare cylindrical reactor with extrapolated height $(\tilde{H})$ is a cosine functional. Thus we can assume $q'(z) = q'_{FE} \times F_{tot}^{P} \times cos\left(\frac{\pi}{\tilde{H}} z\right)$.

Once again, the heat transfer equations are solved analytically for each region in the axial direction under the same assumptions.

$$T_b(z) = T_{in} + \frac{q'_{max}}{\omega C_p} \times \left(\frac{\tilde{H}}{\pi}\right) \times \left[sin\left(\frac{\pi}{\tilde{H}}z\right) + sin\left(\frac{\pi H}{2\tilde{H}}\right)\right],$$

$$T_{CO}(z) = T_{in} + q'_{max} \times \left[\frac{\tilde{H}}{\pi\omega C_p} \times \left\{sin\left(\frac{\pi}{\tilde{H}}z\right) + sin\left(\frac{\pi H}{2\tilde{H}}\right)\right\} + \frac{1}{2\pi h r_{CO}} \times cos\left(\frac{\pi}{\tilde{H}}z\right)\right],$$

$$T_{CI} = T_{CO}(z) + \frac{q'_{max}}{2\pi k_C} \times ln\left(\frac{r_{CO}}{r_f}\right) \times cos\left(\frac{\pi}{\tilde{H}}z\right),$$

$$T_F(z) = T_{in} + q'_{max} \times \left[\frac{\tilde{H}}{\pi\omega C_p} \times \left\{sin\left(\frac{\pi}{\tilde{H}}z\right) + sin\left(\frac{\pi H}{2\tilde{H}}\right)\right\} + \Delta T_{FE} cos\left(\frac{\pi}{\tilde{H}}z\right)\right],$$

$$\text{where } \Delta T_{FE} = \frac{1}{2\pi h r_{CO}} + \frac{1}{2\pi k_C} \times ln\left(\frac{r_{CO}}{r_F}\right) + \frac{1}{2\pi k_G} \times ln\left(\frac{r_{CI}}{r_F}\right) + \frac{1}{4\pi k_f}$$

Figure 30 shows the fuel element axial temperature distributions.

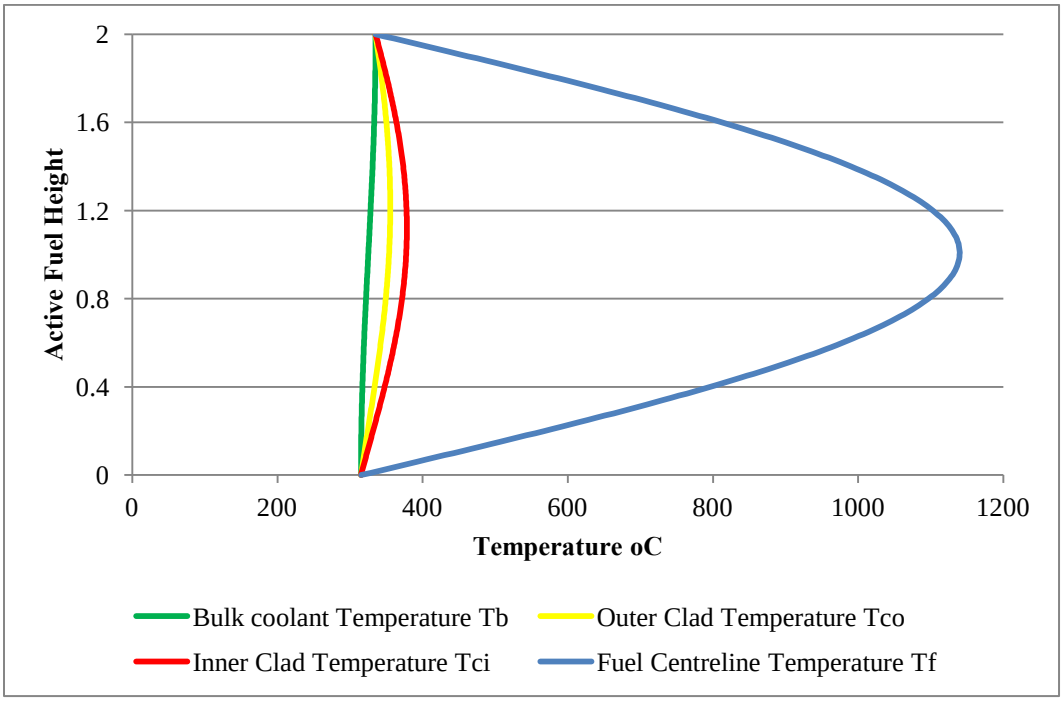

Figure 30: Fuel Element Axial Temperature Distributions

The peak fuel centerline temperature was calculated as ~1140°C; well below the melting temperature of uranium dioxide at ~2800°C (Hausner, 1964). This represents a very large safety margin. The maximum temperature at the outer surface of the cladding was calculated as ~356°C. Again this value is well below the limit in accident scenarios specified in the Code of Federal Regulations (10CFR50.46, 2007) at ~1200°C and represents a large safety net. Both values are not atypical of temperatures experienced in existing large PWRs and as cause no cause for concern regarding the SMR design.

5.3. Critical Heat Flux and Departure from Nucleate Boiling Ratio

The Critical Heat Flux (CHF) is the value for the surface heat flux which corresponds to the upper limit of the nucleate boiling heat transfer regime on the boiling curve. At and above this value for the surface heat flux, the heat transfer regime shifts from nucleate boiling to film boiling. This transition is accompanied by a large drop in the heat transfer rate at the surface.

In the nucleate boiling regime, the entire heating surface (in this case the fuel element cladding) is completely in contact with the coolant. The heat addition causes nucleation at certain sites where conditions are favorable resulting in boiling. The gas bubbles quickly detach or collapse, allowing the liquid coolant to re-contact the clad surface. Heat transfer is largely due to conduction and convection and is at a maximum in this regime. Nuclear reactors aim to operate in the nucleate boiling heat transfer regime. If the CHF is exceeded, the heat transfer regime transitions quickly to film boiling.

In the film boiling regime, a thin film of vapor covers the entire surface of the clad at all times and does not allow the liquid coolant to re-contact the clad surface. Now the major mechanism of heat transfer is by radiation resulting in low heat transfer and high clad surface temperatures (Collier and Thome, 1972; Cheng and Muller, 2003)

The consequences of exceeding the CHF in a nuclear reactor are very severe. Before the CHF point, increasing surface heat flux is accompanied by increased surface heat transfer and increased power output. Exceeding the CHF however places the clad in a situation where it is experiencing an increased surface heat flux and reduced surface heat transfer. The high

clad surface temperatures that result will eventually lead to swelling, blistering, cracking and eventually melting of the clad surface.

The Departure from Nucleate Boiling Ratio (DNBR) is a ratio of the critical heat flux to the actual heat flux at any point along the axial length of the fuel pin at the clad surface. The Westinghouse W-3 correlation for non-uniform axial heat flux in bundle geometry is used to calculate the axial CHF distribution and along with the analytically determined axial distribution for the clad surface heat flux, the DNBR is calculated for the hottest fuel element.

The Westinghouse W-3 correlation (Cheng and Muller, 2003) is

$$CHF_{non-uniform}(z) = \frac{CHF_{uniform}(z)}{F(z)}$$

where $CHF_{non-uniform}(z)$ is the non-uniform CHF, $CHF_{uniform}(z)$ is the uniform CHF, $F(z)$ is the F-correction factor for heat and mass transfer effectiveness at the bubble-layer/sub-cooled liquid-core interface. ($C(z)$ is the C-correction). P is the system pressure, G is the mass flux, i is the enthalpy, D_{FC} is the flow channel equivalent diameter and χ_s is the equilibrium or static quality.

$$\begin{aligned}\mathrm{CHF_{uniform}(z)} = &\left\{2.022 - 0.06238\mathrm{P} + (0.1722 - 0.01427\mathrm{P})\mathrm{e}^{[18.177-0.5987\mathrm{P}]\chi_{s(z)}}\right\} \\ &\times \left[\left(0.1484 - 1.596\chi_s(\mathrm{z}) + 0.1792\chi_s(\mathrm{z})\left|\chi_s(\mathrm{z})\right|\right) \times 2.326\mathrm{G} + 3271\right] \\ &\times \left[1.157 - 0.869\chi_s(\mathrm{z})\right] \times \left[0.2664 + 0.8357\mathrm{e}^{(124.1\mathrm{D_{FC}})}\right] \\ &\times [0.8258 + 0.0003413 \times (\mathrm{i_f(z)} - \mathrm{i_{in}})]\end{aligned}$$

$$\mathrm{F(z)} = \frac{\mathrm{C(z)} \times \int_0^{\mathrm{z}} \mathrm{q''(u)e^{-C(z-u)}du}}{\mathrm{q''(z)} \times (1 - \mathrm{e^{-C(z)}})}$$

$$\mathrm{C(z)} = 185.6 \times \frac{[1-\chi_s(\mathrm{z})]^{4.31}}{\mathrm{G}^{0.478}}$$

Figures 31, 32, 33 and 34 show the variation of the heat flux, the equilibrium quality, the non-uniform critical heat flux and the DNBR with active fuel length respectively.

From these plots we see first that the shape of the heat flux is the same as that of the fuel axial temperature distributions; owing to the cosine functional in the axial spatial distribution of the neutron flux in the core.

Second, the thermodynamic quality is negative for the entirety of the active fuel length. This indicates that the void fraction in the coolant remains negative and there is no two-phase flow expected in the bulk coolant. This does not mean that hot spots and prime nucleation sites on the clad surface will not lead to some nucleate boiling.

Third, for large sections of the active fuel length, the non-uniform critical heat flux is an order of magnitude larger than the actual heat flux. The non-uniform critical heat flux is the heat flux required to have the transition from nucleate boiling to film boiling for the conditions at each axial position.

Most importantly, the DNBR is always above 1. This shows clearly there are no points along the active fuel length with the critical heat flux conditions exceeded. Figure 35 shows a close-up view of the DNBR. In fact the DNBR is greater than 2.94 at all points along the active fuel length; a significant safety margin.

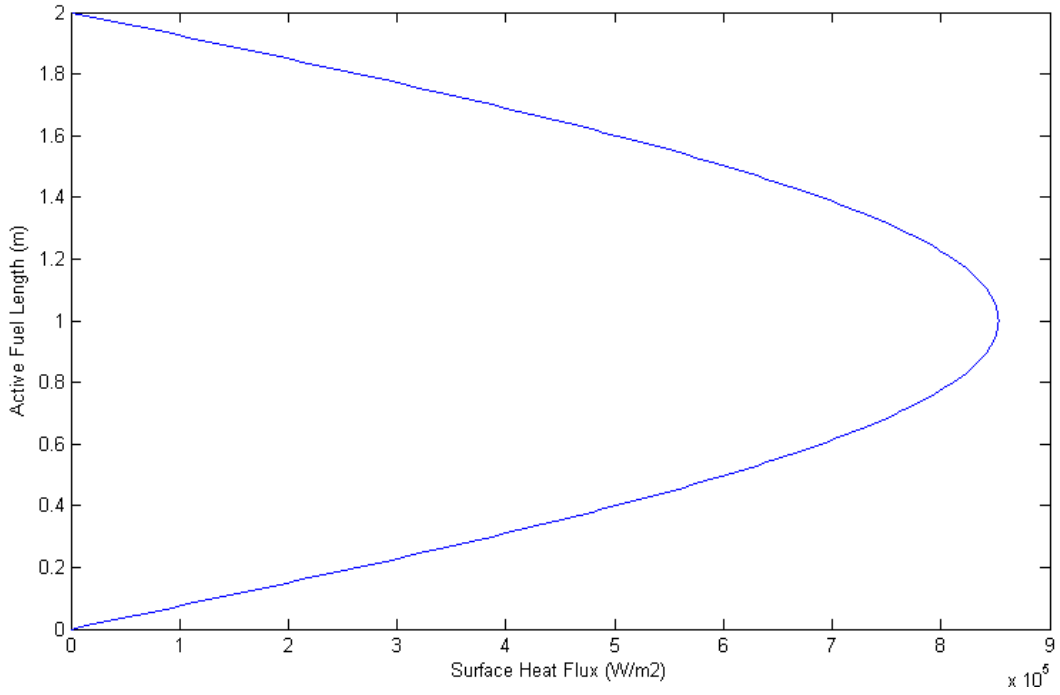

Figure 31: Surface Heat Flux

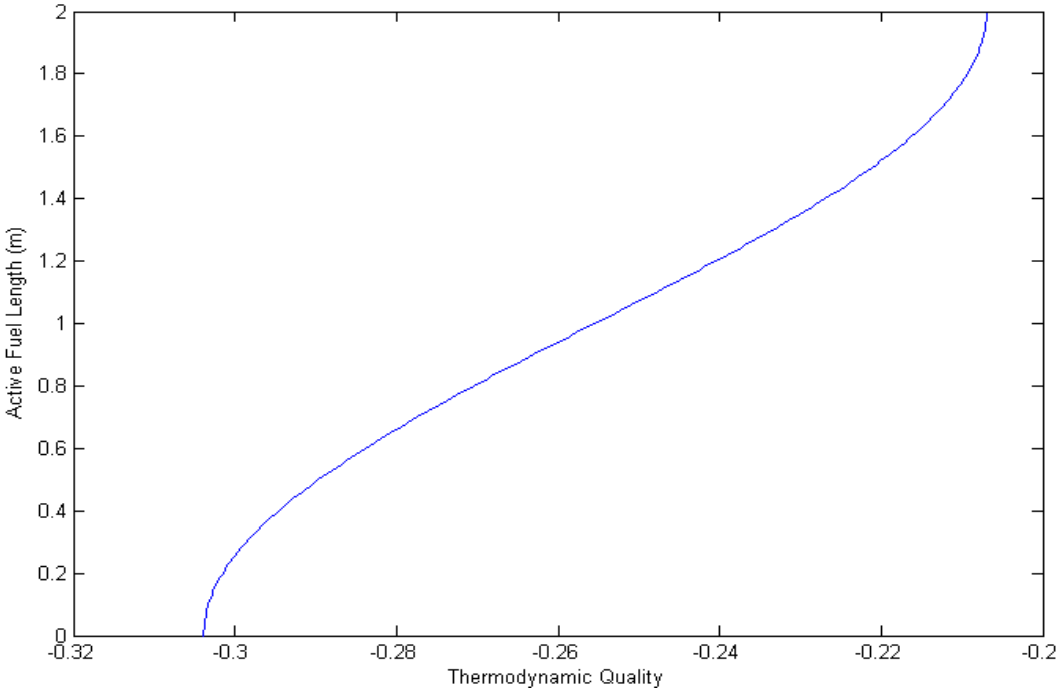

Figure 32: Thermodynamic Quality

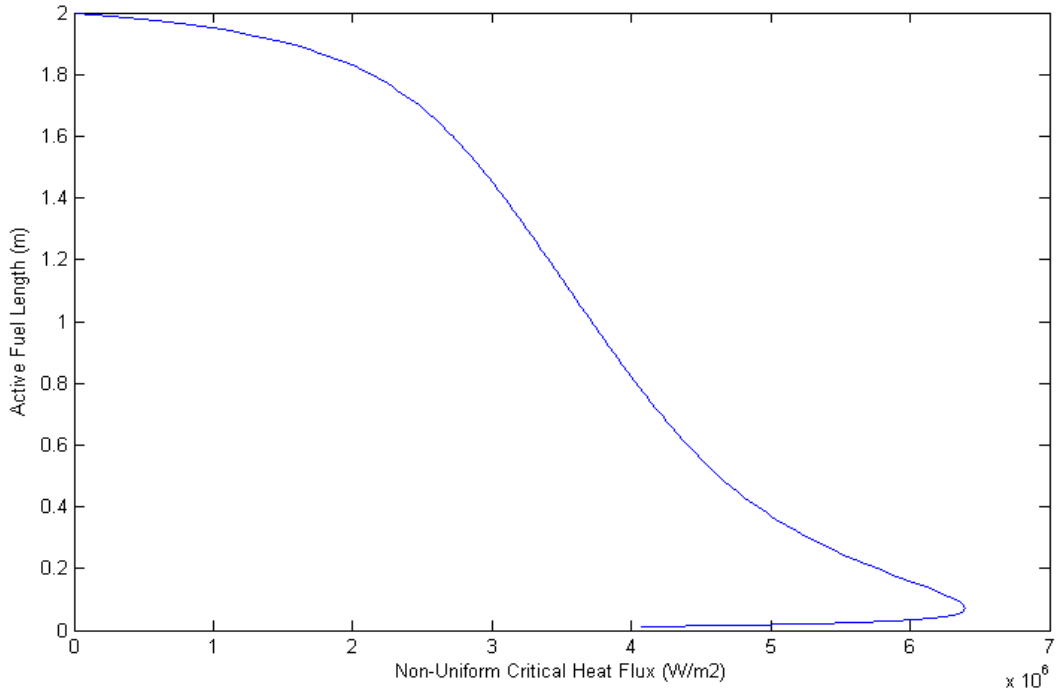

Figure 33: Non-Uniform Critical Heat

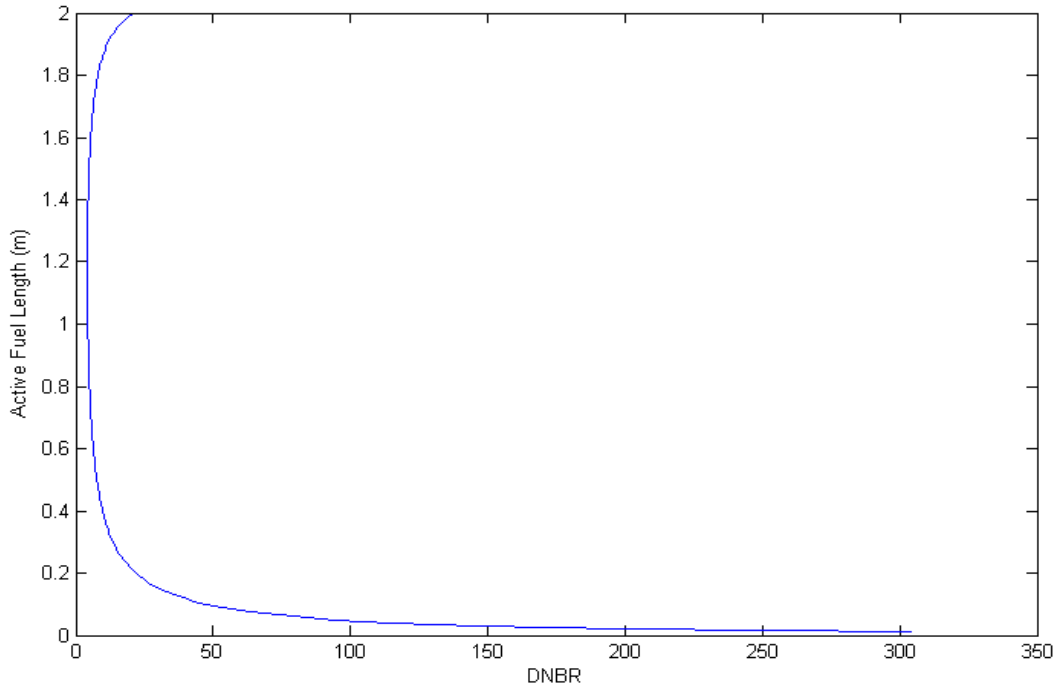

Figure 34: Departure from Nucleate Boiling Ratio

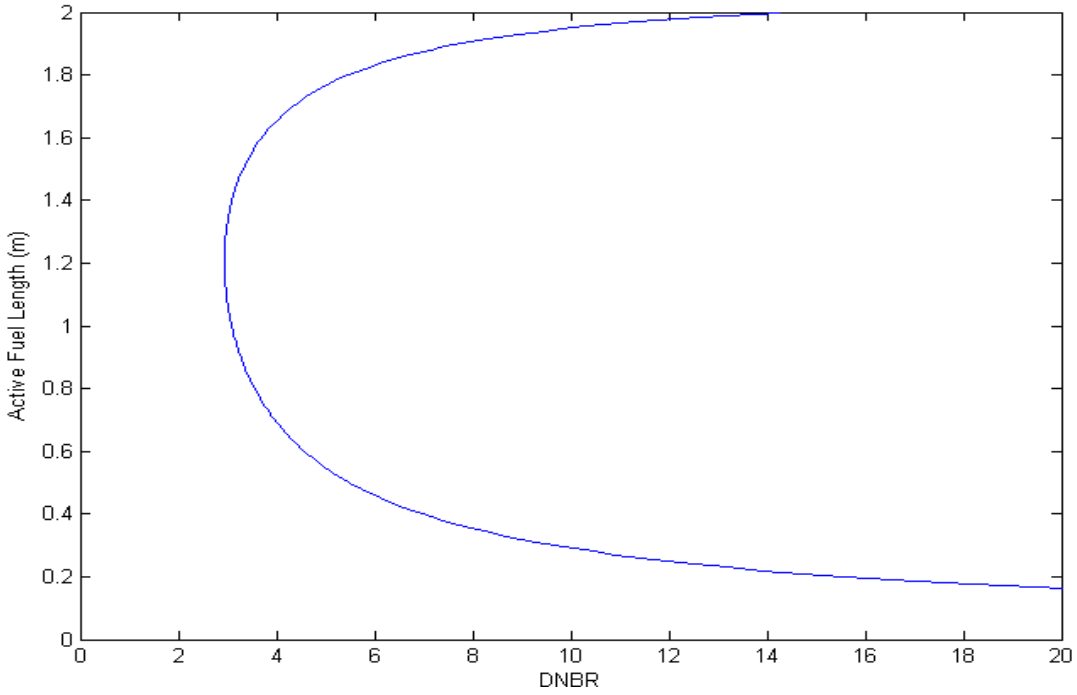

Figure 35: Close-up View of Departure from Nucleate Boiling Ratio

6. PROLIFERATION RESISTANCE

Proliferation Resistance (PR) as defined by the IAEA is the characteristics of a nuclear system that impedes diversion or undeclared production of nuclear material, or misuse of technology, by States in order to acquire nuclear weapons or other nuclear explosive devises (IAEA, 2002). In the past, PR of nuclear reactors was not a major concern as most reactors were situated inside recognized weapons states. With the advent of the spread of nuclear technology, came an increased attention to PR. The PR of nuclear reactors in particular has become increasingly more important.

The financial capital barrier that accompanied the larger 1000MWe+ nuclear reactors that hindered the spread of nuclear technology and restricted them largely to developed nations will be removed by SMRs and as such nuclear technology in the shape of SMRs will become accessible to developing nations. In general, safeguards and safety procedures in this new market for nuclear reactors is not to the same level as that of the developed nations. As such, much emphasis has been placed on developing inherently proliferation resistant characteristics and incorporating them into newer reactor designs.

As a result, a proliferation resistance assessment was performed on the optimized SMR design developed in the proceeding chapters to evaluate the proliferation resistance characteristics of the SMR relative to that of an existing large PWR.

6.1. Multiple Attribute and Utility Analysis

The computer code used to perform the PR assessment is the Proliferation Resistance Analysis and Evaluation Tool for Observed Risk (PRAETOR). PRAETOR was developed at Texas A&M University by its Nuclear Security Science and Policy Institute (NSSPI) for the purpose of aiding in the analysis of nuclear facilities having nuclear material that can be diverted for the purpose of fabricating a nuclear weapon or explosive device. The code uses Multi Attribute Utility Analysis (MAUA) to provide a single metric for an installation based 63 intrinsic and extrinsic characteristics of the nuclear material available and the facility in question.

Multi Attribute Utility Analysis provides a methodology by which several factors or attributes affecting a single characteristic; in this case the proliferation resistance of the facility can be combined into a single representative metric. This is done by assigning a utility value between 0 and 1 to each attribute to be considered using utility mapping functions. The utility mapping functions are carefully developed to reflect the PR value added by having a certain value for each attribute. Each attribute is also assigned an expert determined weight. The weights indicate the relative importance of the attributes relative to one another and were established from a survey of over 100 nuclear non-proliferation experts, nuclear engineers, scientists/engineers and policy experts. The general form of the multi attribute utility function is

$$U\left(x_1, x_2, ..., x_n\right) = \sum_{i=1}^{n} k_i u_i\left(x_i\right) + K\sum_{\substack{i=1 \\ j>i}}^{n} k_i k_j u_i\left(x_i\right) u_j\left(x_j\right) + K^2 \sum_{\substack{i=1 \\ j>i \\ l>j}}^{n} k_i k_j k_l u_i\left(x_i\right) u_j\left(x_j\right) u_l\left(x_l\right) + ...$$

$$.....+ K^2 k_1 k_2 ... k_n u_1\left(x_1\right) u_2\left(x_2\right) .... u_n\left(x_n\right)$$

where $x_1, x_2 ....., x_n$ are the individual attributes, $u_1\left(x\right), u_2\left(x\right) ...., u_n\left(x\right)$ are the utility functions for the attributes $x_1, x_2 .....x_n$ and $k_1, k_2, ..., k_n$ are the expert defined weights associated with the $K^2 k_1 k_2 ... k_n u_1\left(x_1\right) u_2\left(x_2\right) .... u_n\left(x_n\right)$ attributes. K is a scaling parameter and $U\left(x_1, x_2, ..., x_n\right)$ is the overall single metric for the system under consideration. The scaling parameter K must be > -1 and satisfy the condition

$$1 + K = \prod_{i=1}^{n}\left(1 + K k_i\right)$$

6.2. Inputs to PRAETOR

The PRAETOR code required the user to input values for each of the 63 attributes used for the MAU analysis it performs. The analysis is performed on three separate tiers. The 63 attributes are firstly folded into 11 subgroups and a PR values assigned to each subgroup; this is tier one. The 11 subgroups are then folded into the four major stages of the diversion process; this is tier two. The values for the four stages are finally folded into the single PR metric for the entire system in tier three. A list of the 63 attributes can be found in the PRAETOR manual (Chirayath et al., 2010).

6.3. Diversion Scenario and Key PRAETOR Inputs

6.3.1. Diversion Scenario

The diversion scenario simulated in this portion of the work aimed to analyze the ease with which spent fuel (SF) assemblies from the proposed SMR could be diverted for the purposes of manufacturing a nuclear weapon or explosive device.

Under the proposed deployment schemes for the new fleet of SMR's, onsite storage in fuel pools is discarded in favor of transporting the irradiated material back to the a post-irradiation processing plant either at the factory where the fuel is produced or on some other site. This operation scheme, if attainable drastically increases the proliferation resistance of the SMR site when compared to a large commercial PWR plant in the US, some of which have fuel pools holding SF inventories dating back to 30years of operation.

In order to allow comparison with the current deployment of commercial PWRs in the US, a comparison is made between two spent fuel storage (SFS) facilities; one storing SF assemblies from a single 1000MWe PWR and the other storing SF from 5 SMRs also producing a combined 1000MWe. Both facilities are assumed to be situated in the same country thus the values for the PRAETOR inputs regarding country characteristics and weapons capabilities will be the same.

In this way, the comparison is made between intrinsic properties of the reactor and its fuel and does not reflect specific details of the PWR and SMR installations such the actual

layout of the plant, physical security systems such as guards, fences and cameras and other such variables which are beyond the capability of the PRAETOR code.

6.3.2. Key PRAETOR Inputs

For the specified diversion scenario described above, a large number of the PRAETOR inputs are the same for both the SMR plant and PWR plant. Thus those attributes that have different values become key and will in effect determine the relative difference in proliferation resistance between SFS facilities housing assemblies from PWRs or SMRs. Table 16 has a list of the key attributes to determine the relative proliferation resistance for the specified diversion scenario. These characteristics are physical properties of the SF assemblies such as volume, mass, dose rate and heat load of the material.

Immediately we see that the assessment variable are all concerning the diversion and transportation characteristics of the PWR assembly that for the SMR. The question being answered here is, assuming the adversary is able to divert material from both the PWR SFS and SMR SFS, which one would the adversary likely choose due to its lower proliferation resistance. The transformation and weapon fabrication stages are considered identical for the fictitious state.

Table 16: Key PRAETOR Attributes for Diversion Scenario (10years cooled)

Major Stage	Attribute Name	SMR	PWR
Diversion	1. Mass/significant quantity(SQ), of nuclear material diverted (kg)	902.72	1094.73
	2. Volume/SQ of nuclear material diverted (m3)	0.102	0.119
	3. Number of items per SQ (number)	4	2
	5. Radiation level in terms of dose (Sv/hr)	50.49	46.22
	8. Heat load of nuclear material (watts/cc)	0.0102	0.0213
	12. Amount of nuclear material available (number of SQs)	170	180
Transportation	23. Mass/significant quantity(SQ), of nuclear material diverted (kg)	902.72	1094.73
	24. Volume/SQ of nuclear material diverted (m3)	0.102	0.119
	26. Radiation level in terms of dose (Sv/hr)	50.49	46.22
	27. Heat Load of nuclear material	0.0102	0.0213
	31. Mass of material and transportation container (kg)	20000	25000
	32. Volume of material and transportation container (m3)	6.362	16.040
	33. Heat load of nuclear material (watts/cc)	4.09E-05	1.58E-04
	34. Shield thickness needed to reduce dose rate to 10mR/hr (m of Pb)	0.570	0.566

6.4. ORIGEN-ARP Calculation with Outputs from MCNP and MCNPX

ORIGEN-ARP is employed to perform fuel depletion (only for PWR case) and decay calculations and produce radiation and heat load data for both the PWR and SMR. The source term data in the ORIGEN-ARP output is used to generate a MCNP model to calculate the expected neutron and photon dose rates from the SF assemblies as a function of decay/cooling time. This data is also used as PRAETOR input to perform the PR analysis.

6.5. Proliferation Resistance Analysis

The utility values for the SMR and PWR for the Diversion and Transportation Stages in the second tier of the MAUA are presented in Table 17. Figure 36 and Figure 37 shows the data for the Diversion and Transportation stage respectively.

Table 17: Relative PR Values for Diversion and Transportation Stages

Cooling Time (years)	SMR Diversion	SMR Transportation	PWR Diversion	PWR Transportation
0.01	0.643	0.507	0.647	0.537
0.03	0.641	0.501	0.645	0.531
0.1	0.640	0.497	0.643	0.524
0.3	0.640	0.497	0.641	0.517
1	0.640	0.495	0.641	0.514
3	0.640	0.494	0.641	0.513
5	0.640	0.494	0.641	0.512
10	0.640	0.493	0.641	0.512

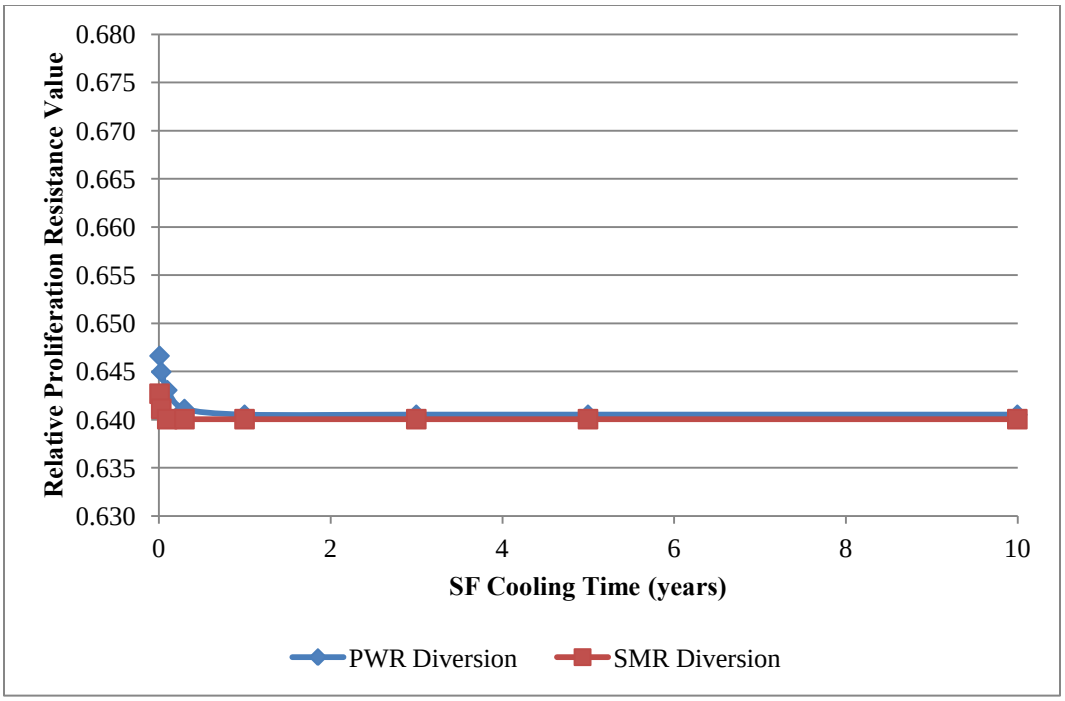

Figure 36: Relative PR Value at Diversion Stage

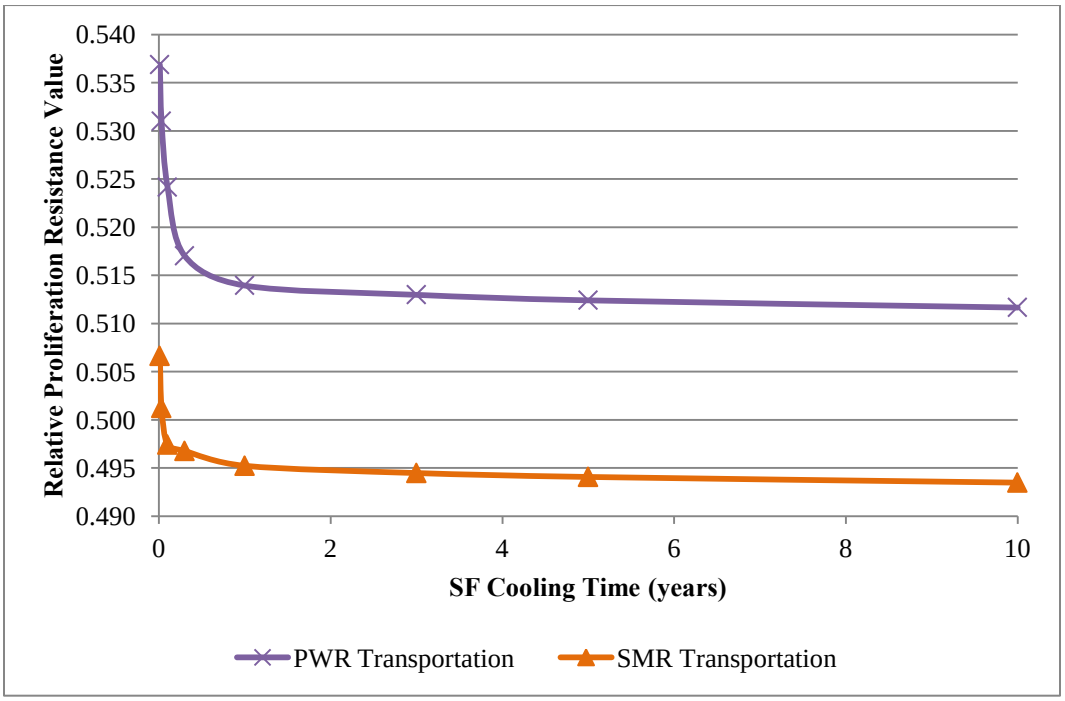

Figure 37: Relative PR Value at Transportation Stage

From these results we see that the difficulty in diverting the required material (2 PWR assemblies or 4 SMR assemblies) from their respective storage facilities is essentially the same. For the Transportation stage, we see a small but more pronounced difference, with the smaller more compact SMR assemblies easier to transport and hence have a lower PR value.

The third tier results for the overall PR value are presented in Table 18. From the PRAETOR results we see that the PWR SFS has a higher overall PR value. This is a result of higher PR values regarding diverting and transporting the material; the major contributor being the transportation stage. Considering the raw input data (Table 16), this is to be expected. Two PWR assemblies need to be diverted as compared to four SMR assemblies. This is a positive for the SMR however the larger length, volume and mass of the PWR assemblies make them more difficult to divert overall. This coupled with higher values for heat load and radiation dose result in a much greater handling difficulty and shielding requirements for the PWR fuel. The higher heat load and radiation dose are a direct result of the PWR assemblies seeing a higher average burnup; an average of 55GWd/MTU as opposed to an average of 40GWd/MTU for the SMR.

In addition, the lower burnup of the SMR assemblies produces a higher quality of plutonium vector than the more depleted PWR. This variable is not captured in PRAETOR.

Saying this however, the proper conclusion regarding the relative proliferation resistance on the SFS installations is that they are in fact the same. The values for the SMR and PWR SF assemblies are in fact statistically equivalent with a less than 1.5 percent difference in all the values. Table 18 shows the overall PR values and the resultant percent difference values. The actual difference in the values is not large enough for a high level decision maker to make a clear determination as to which system is more at risk to a proliferation attempt. Figure 38 allows for this conclusion to be clearly seen.

Table 18: Relative Overall PR Value

Cooling Time (years)	SMR Overall PR Value	PWR Overall PR Value	Percent Difference
0.01	0.479	0.486	1.448
0.03	0.477	0.484	1.45
0.1	0.476	0.482	1.24
0.3	0.476	0.480	0.83
1	0.476	0.479	0.63
3	0.476	0.479	0.63
5	0.476	0.479	0.63
10	0.476	0.479	0.63

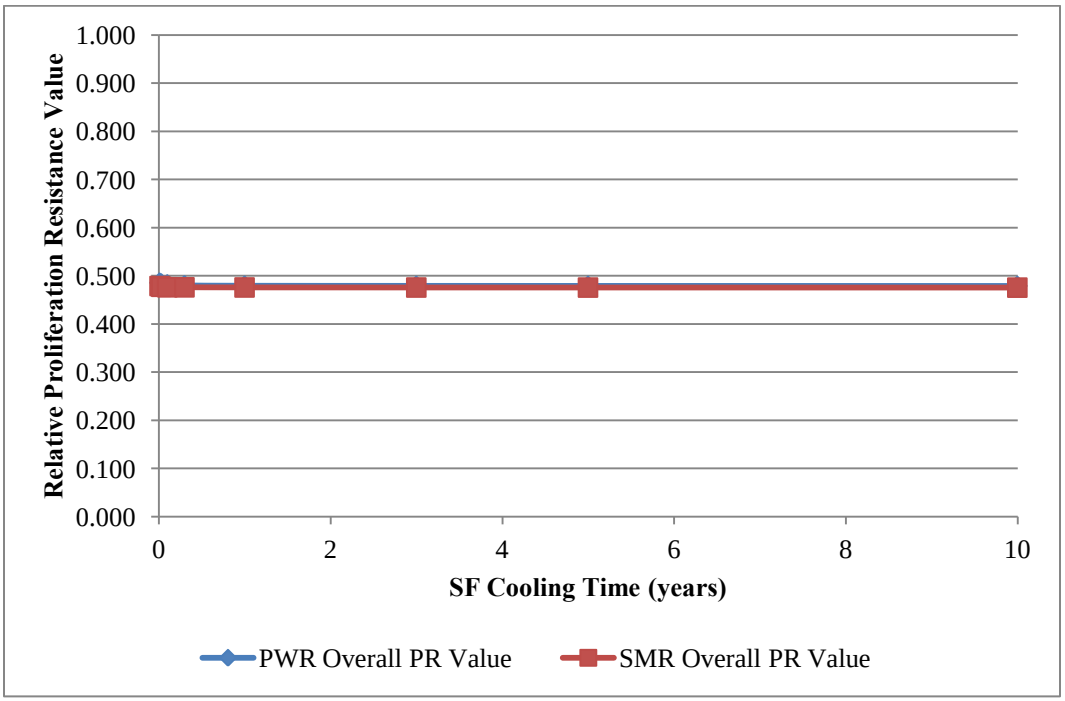

Figure 38: Relative Overall PR Value

7. CONCLUSIONS AND FUTURE DEVELOPMENTS

7.1. Conclusions

With the advent of the second nuclear era, small modular reactors stand poised to play an important role in ushering in this era. With near-term deployment a driving goal, an SMR design of the integrated pressurized water reactor type was chosen for the study. Publicly available information (Dec 2010) regarding the mPower SMR from Babcock & Wilcox (B&W) and existing large PWR parameters were used to mould a set of design goals and constraints. The goals for the work was to develop and analyze a computational model of an SMR core producing 500MWth with a four year core lifetime with enrichment less than 5% ^{235}U for an average fuel burnup of 40GWd/MTU. These goals along with safety parameter evaluations were pursued in this study.

1. Fuel assembly dimensions were kept the same as that of an existing large PWR with the aim of facilitating expedient licensing of the SMR design. To obtain the small core of an SMR design, investigations regarding the effect of decreasing the active fuel length of the existing large PWR assembly on the effective multiplication factor revealed that a minimum fuel length of 180cm was required. In order to achieve a core inventory of uranium capable of sustaining the 500MWth output for four years an active core length of 200cm was selected.
2. The desire for a small core size coupled with restrictions regarding the core height-to-diameter ratio from neutronics considerations yielded a core layout with 69 assemblies. The resulting core arrangement resulting in an equivalent diameter of 194.5cm.
3. Decisions regarding the core loading pattern employed acquired increased importance as design constraints restricted core shuffling and the use of boric acid dissolved in the coolant. Thus reactivity control and uniform core burnup had to be achieved by a precise combination of initial core loading and positioning of burnable absorber rods (BARs).

4. Various fuel enrichments (3.6, 4.0, 4.4, 4.8 and 5% ^{235}U) were considered in the determined core layout, with results of bare core depletion simulations indicating that a primary enrichment (PE) of at least 4.8% ^{235}U was required to attain the desired core lifetime. The addition of assemblies enriched to 4.4% ^{235}U at the centre of the core and BARs to control peaking behavior necessitated the use of a PE of 4.95% ^{235}U.
5. Optimization of the number and position of BARs within the peaking assemblies was employed to attain a favorable BAR loading pattern. This optimized pattern resulted in a radial and axial power peaking factor of 1.24 and 1.09 respectively, for a total power peaking factor of 1.35.
6. The optimized core configuration resulted in a core lifetime of 1270days at full power, a capacity factor of 0.87. An average burnup of 48.93GWd/MTU and 38.58GWd/MTU was achieved for the primary and secondary enriched assemblies respectively for a core wide average fuel burnup of 38.77GWd/MTU.
7. Analysis of the isotopic composition of the spent fuel showed consistency with literature regarding the amount of plutonium produced and the overall radioactivity of the assembly for the levels of burnup achieved. On average 2.11kg of plutonium was produced in the PE assemblies.
8. The calculated power peaking factors were utilized in the thermal hydraulics assessments and found to be acceptable for safe operation of the reactor. Reactor kinetics parameters were also calculated and found to be typical of LEU PWR systems. This result engenders confidence in the safe operation of the reactor leveraging the years and years of experience with large PWRs as the SMR is anticipated to behave in a similar fashion.
9. Reactivity coefficients were found to be negative for the fuel temperature, moderator temperature, void and power indicating self limiting transients and an inherently safe reactor design.
10. An analytical thermal hydraulics assessment was done using the power profiles and peaking factors determined in the neutronics analysis. Fuel temperature distributions were calculated for the fuel element in both the radial and axial directions. The peak fuel centerline temperature was calculated as ~1140°C; well below the melting

temperature of uranium dioxide at ~2800°C and the maximum temperature at the clad outer surface was found to be ~356°C. Both values have significant safety margin and are a source of confidence concern regarding the performance safety of the SMR design.

11. The fuel clad surface heat flux is calculated and the non-uniform Critical Heat Flux is calculated using the Westinghouse W-3 correlation. The departure from nucleate boiling ratio is determined and found to be well above unity for the entire active fuel length. As such the SMR is shown to operate in a heat flux regime under which conditions for "dry out" cannot be attained and associated undesirable phenomena such as boiling of the coolant and swelling, blistering and eventual melting of the cladding is avoided.
12. Using the data for isotopic composition of the fuel material and heat load and radiation dose expected from the SMR fuel assembly and a typical PWR fuel assembly a proliferation resistance analysis was done using the PRAETOR code on a scenario whereby an adversary wished to divert spent fuel material. Results of the analysis showed that the SMR and PWR assemblies had the same PR value. This was as expected as the key parameters in the analysis were functions of material for which the PWR and SMR are closely related i.e. LEU fuel less than 5%235U content, depleted in a PWR thermal spectrum to a similar level of burnup.
13. Through the development of the core model, it has been clearly shown that the performance targets set for the SMR cannot be attained with a 200cm active fuel length. Information released by mPower (June 2012) confirmed these findings. The new information described an mPower SMR with an active fuel length 240cm rated at 530MWth. Depletion calculations were executed to confirm the findings of this work and determine whether the original targets are attained under these new design parameters. The new results showed that a core lifetime of 1400days is easily attainable and with core lifetime extension measures, the SMR is fully capable of 4years of full power operation.

In conclusion, a viable configuration model for the reactor core of a SMR of the IPWR type has been developed and analyzed and proven to show favorable characteristics. The design goals of attaining a small core producing 500MW of thermal energy output for four years has been achieved at a capacity factor of 0.87 with room for improvement of this value to 0.9. This has been done under the constraints of LEU fuel with enrichment less than 5% ^{235}U. From a thermal hydraulics standpoint, the design is shown to be fundamentally sound with results of fuel temperature, CHF and DNBR analyses showing an inherently safe and viable design. In terms of proliferation resistance, it has been demonstrated using multi attribute utility analysis theory that the SMR spent fuel possesses the same level of proliferation resistance as spent fuel from the existing fleet of PWRs. This work serves as a solid foundation, on which future efforts looking to further develop and optimize the design can be laid.

7.2. Future Work

Initial efforts have resulted in the development of a viable design for a small modular integral pressurized water reactor. These efforts serve as ground work on which future efforts can stand. Substantial work remains to be done to arrive at a fully fledged design. This work should look to encompass further neutronics analysis, a more robust thermal hydraulics assessment, coupling of the neutronics and thermal hydraulics phenomena to understand feedback effects and time dependent reactor behavior, design and optimization of the balance of plant components, a safety analysis and a detailed study of economics considerations.

Improved core lifetime and fuel utilization can be achieved by further flattening of the core power profile. Apart from further optimization of the techniques previously used, other avenues such as a third enrichment level, fuel integral burnable absorbers and enrichment zoning whereby there is axial variation in fuel enrichment all remain unexplored. Implementations of these schemes would also result in a more accurate model and increase accuracy of the results.

It is likely that the control rod material and design used in existing large PWRs and their associated drives and mechanisms should be directly transferable to the SMR. This results from the assembly dimensions, materials and configurations remaining unchanged.

Nevertheless methods for controlling the reactor should be investigated and proven to be sufficient for the start-up, operation and effective shut down of the core and if possible, more efficient methods found.

Further thermal hydraulics assessments would require more robust models. These models should serve to remove many of the assumptions that were necessitated to allow for analytical solutions such as constant densities, thermal conductivities etc. Three-dimensional temperature profiles for the fuel, gap, clad and coolant would allow for more accurate neutronics and thermal hydraulics. These can be obtained by employing existing coupled neutronics and thermal hydraulics codes such as RELAP5 or the use of computational fluid dynamics (CFD). A key goal in this study should be to determine the role that natural circulation could play in terms of heat removal and inherent safety of the core in accident scenarios.

Coupled neutronics and thermal hydraulics provides a means whereby transient analysis can be performed to understand the time dependent behavior of the core and reactor in non-steady state conditions.

Components of the Balance of Plant for the IPWR required more consideration and optimization bringing into effect another feedback loop whereby the efficiency of heat removal through the steam generator on the secondary side directly affects the behavior of the reactor core on the primary. Additional components such as feedwater heaters, high and low pressure turbines and regeneration can all be employed to increase the efficiency with which electricity is produced by the power plant. This also requires investigation and optimization.

Once the entire power plant has been designed, safety analysis can then encompass entire accident scenarios. Although the IPWR configuration has eliminated some accident scenarios altogether, those that remain need to be well understood such that all benefits of having a deliberately small reactor are fully exploited.

Finally a study into the economics of the design is required. Regardless of the strengths and aesthetics of a design, financial justification is required if it is ever to see the light of day. In borrowing large portions from existing PWR technology, the IPWR SMR stands at a great advantage in comparison to the more exotic type SMRs thus allowing it to stand alone as the only near-deployment SMR. This is because the technology used makes

the design economically viable in addition to making it readily achievable. The aim of the study should not only look at the cost of construction of the reactor but also identify markets, locations and conditions necessary to justify its construction and make it competitive to an electricity vendor in today's markets.

REFERENCES

Babcock & Wilcox, 2012. Press Release - Generation mPower Snapshot http://www.generationmpower.com/pdf/sp201100.pdf

Carelli, M. D., Garrone, P., Locatelli, G., Mancini, M., Mycoff, C., Trucco, P., Ricotti, M. E., 2010. Economic features of integral, modular, small-to-medium size reactors. Progress in Nuclear Energy, 52 (4) 403-414.

Cheng, X., Muller, U., 2003. Review on Critical Heat Flux in Water Cooled Reactors. Forschungzentrum Karlsruhe GmbH, Karlsruhe.

Chirayath, S. S., Ragusa, J. C., Charlton, W. S., 2010. Proliferation Resistance Analysis and Evaluation Tool for Observed Risk (PRAETOR) Version 1, User Manual, Texas A&M University, College Station, Texas.

Code of Federal Regulations. 10CFR50.46. Acceptance criteria for emergency core cooling systems for light water nuclear power reactors. As amended at 72 FR 49508, August 2007.

Collier J. G. Thome, J. R., 1972. Convective Boiling and Condensation, Second Edition. Clarendon Press, Oxford.

Gauld I.C., Bowman S. M., and Horwedel, J. E., 2009. ORIGEN-ARP Automatic Rapid Processing for Spent Fuel Depletion, Decay and Source Term Analysis. Oak Ridge National Laboratory, Tennessee.

Giannangeli D. D. J. III., 2007. Development of the Fundamental Attributes and Inputs for Proliferation Resistance Assessments of Nuclear Fuel Cycles. Master's Thesis, Texas A&M University. College Station, Texas.

Hausner, H., 1964. Determination of the Melting Point of Uranium Dioxide. Journal of Nuclear Materials, 15, 179-183.

IAEA, 2007. Nuclear Technology Review 2007, International Atomic Energy Agency, Vienna, Austria.

IAEA, 2002. Proliferation Resistance Fundamentals for Future Nuclear Energy Systems. International Atomic Energy Agency, Vienna, Austria.

Ingersoll, D. T., 2009. Deliberately Small Reactors and the Second Nuclear Era. Progress in Nuclear Energy 51 (4-5), 589-603.

Kok, K. D., (Editor) 2009. Nuclear Engineering Handbook, CRC Press, Boca Raton, Florida.

Metcalf, R. R. M., 2009. New Tool for Proliferation Resistance Evaluation Applied to Uranium and Thorium Fuelled Fast Reactor Fuel Cycles. Master's Thesis, Texas A&M University. College Station, Texas.

Muhammad, F., 2010. Kinetic parameters of a low enriched uranium fuelled material test research reactor at end-of-life. Annals of Nuclear Energy (37) 10, 1411-1414.

Pelowitz, D. B., (Editor) 2008. MCNPX User's Manual. Los Alamos National Laboratory, Los Alamos, New Mexico.

Shirvan K., Hejklar P., Kazimi M., 2012. The Design of a Compact Integral Medium Size PWR. Nuclear Engineering Design 243, 393-403

USNRC. 2011. Briefing on Small Modular Reactors (Transcript of proceedings). United States Nuclear Regulatory Commission, Washington DC, USA.

Westinghouse Electric Co., LLC 2003a. AP1000 Design Control Document Chapter 4. Cranberry, Pennsylvania.

Westinghouse Electric Co., LCC 2003b. AP1000 Plant Description. Cranberry, Pennsylvania.

X-5 Monte Carlo Team, 2008. MCNP: A General Monte Carlo N-Particle Transport Code, Version 5 Volume I & II: Overview and Theory. Los Alamos National Laboratory. Los Alamos, New Mexico.